

JAERI - M
87-135

PIPE RUPTURE TEST RESULTS : CROSS-OVER
LEG PIPE WHIP TEST UNDER PWR LOCA
CONDITIONS (RUN 5808, 5809)

September 1987

Ryoichi KURIHARA, Shuzo UEDA Toshikuni ISOZAKI
Rokuro KATO, Kiyoshi KATO and Shohachiro MIYAZONO

日 本 原 子 力 研 究 所
Japan Atomic Energy Research Institute

JAERI-Mレポートは、日本原子力研究所が不定期に公開している研究報告書です。
入手の問い合わせは、日本原子力研究所技術情報部情報資料課（〒319-11茨城県那珂郡東海村）あて、お申しこしてください。なお、このほかに財団法人原子力弘済会資料センター（〒319-11 茨城県那珂郡東海村日本原子力研究所内）で複写による実費頒布をおこなっております。

JAERI-M reports are issued irregularly.

Inquiries about availability of the reports should be addressed to Information Division
Department of Technical Information, Japan Atomic Energy Research Institute, Tokai-mura, Naka-gun, Ibaraki-ken 319-11, Japan.

©Japan Atomic Energy Research Institute, 1987

編集兼発行 日本原子力研究所
印刷 網高野高速印刷

Pipe Rupture Test Results : Cross-Over Leg Pipe Whip
Test under PWR LOCA Conditions (RUN 5808, 5809)

Ryoichi KURIHARA, Shuzo UEDA
Toshikuni ISOZAKI, Rokuro KATO
Kiyoshi KATO and Shohachiro MIYAZONO

Department of Reactor Safety Research
Tokai Research Establishment
Japan Atomic Energy Research Institute
Tokai-mura, Naka-gun, Ibaraki-ken

(Received August 11, 1987)

A series of pipe rupture tests has been performed at the Japan Atomic Energy Research Institute (JAERI) to demonstrate the safety of the primary coolant circuits in the event of pipe rupture, in nuclear power plants. The present report summarizes the results of cross-over leg pipe whip tests (RUNs 5808, 5809), under PWR LOCA conditions (325 °C, 15.7 MPa), which were performed in April, 1984.

The cross-over leg pipe whip test was performed to demonstrate the integrity of the restraints at the LOCA by using a 1/6 model of piping in the PWR nuclear power plants. Strain-gages, accelerometers and load cells were used to measure the dynamic response of the test pipe. Test results showed that the deformation of the restraints were within elastic region, and the residual deformation at the free end of pipe was within 10 mm.

Keywords: Pipe Whip, Cross-Over Leg, PWR LOCA, 1/6 Model, Restraint,
Rupture Disk

This work was performed under the contract between the Science and Technology Agency of Japan and JAERI to demonstrate the safety against pipe rupture of the primary coolant circuit in nuclear power plants.

配管破断試験：PWR・LOCA条件下のクロスオーバーレグ
パイプホイップ試験（RUN 5808, 5809）

日本原子力研究所東海研究所原子炉安全工学部

栗原 良一・植田 脩三・磯崎 敏邦

加藤 六郎・加藤 潔・宮園昭八郎

（1987年8月11日受理）

日本原子力研究所では、一連の配管破断試験を軽水炉の配管破断事故時に一次冷却系の構造安全性を実証するために実施している。本報は、1984年4月に実施したPWR-LOCA（325℃，1.5.7 MPa）下のクロスオーバーレグパイプホイップ試験の結果をまとめたものである。

クロスオーバーレグパイプホイップ試験はPWR型原子炉配管系の1/6モデルを用いて、LOCA時におけるレストレントの健全性を実証するために実施された。ひずみゲージ，加速度計およびロードセルを配管試験体の動的挙動を計測するために使用した。試験結果から，レストレントの変形は弾性範囲内にあり，配管先端の残留変形量は10 mm以内であることがわかった。

本研究は、原子炉一次冷却系の配管破断に対する安全性を実証するために科学技術庁からの受託研究として実施した結果をまとめたものである。

東海研究所：〒319-11 茨城県那珂郡東海村白方字白根2-4

CONTENTS

1. INTRODUCTION	1
2. TEST PROCEDURE	2
2.1 Test Equipment	2
2.2 Test Condition	2
2.3 Measuring Items and Devices	3
2.4 Test Procedure	4
3. TEST RESULTS	22
3.1 Results of Residual Deformation Measurements	22
3.2 Photographs before and after the Test	22
3.3 Observation of Pipe Whip Movement by High Speed Camera	23
4. DISCUSSION	35
4.1 Time Sequence of the Major Events	35
4.2 Pressure Decrease in the Vessel and the Pipe	35
4.3 Deformation of the Test Pipe	36
4.4 Deformation of Restraint	37
4.5 Acceleration of Test Pipe	37
4.6 Restraint Force	37
5. CONCLUDING REMARKS	43
ACKNOWLEDGEMENTS	43
REFERENCES	43

目 次

1. まえがき	1
2. 試験方法	2
2.1 試験装置	2
2.2 試験条件	2
2.3 測定項目と方法	3
2.4 試験方法	4
3. 試験結果	22
3.1 残留変形測定の結果	22
3.2 試験前後の写真	22
3.3 高速度カメラによるパイプホップ運動の観察	23
4. 考 察	35
4.1 主な事象の時系列	35
4.2 圧力容器と配管における減圧	35
4.3 試験配管の変形	36
4.4 レストレントの変形	37
4.5 試験配管の加速度	37
4.6 レストレント力	37
5. 結 論	43
謝 辞	43
参考文献	43

1. INTRODUCTION

A series of pipe rupture tests has been conducted using FRPC-II* as one of tests for reliability study of pressure boundary components at JAERI. Pipe whip tests are a part of pipe rupture tests, and have been performed under BWR (285 °C, 6.8 MPa) or PWR (320 °C, 15.6 MPa) LOCA conditions using test pipes of 4-, 6- and 8-inch diameter. The 4-inch diameter pipe whip tests^{(1),(2)} had been already reported.

Two different types of tests were performed. One was the cantilever type pipe whip test using the test pipe of 5000 mm in length and U-shaped restraints. The cantilever type pipe whip tests were performed to investigate the influences of the overhang length and the pipe diameter on the pipe whip behavior.

The other was the cross-over leg pipe whip test using 1/6 model of piping in the PWR nuclear power plants. Cross-over leg pipe locates between a primary pump and a steam generator in a primary coolant loop of the PWR plant as shown in Fig. 1.1. This pipe whip test simulated the circumferential guillotine break at the location ④ of Fig. 1.1.

This report presents the results of the latter test, i.e. the cross-over leg pipe whip test, and studies the behavior of the test pipe and the restraints.

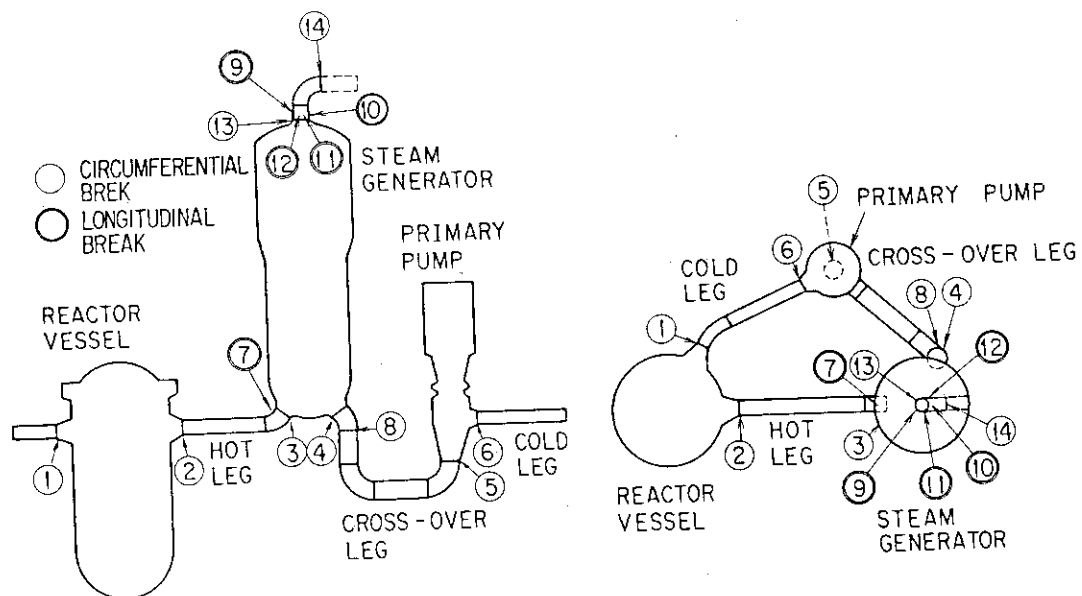


Fig. 1.1 Primary coolant loop of PWR plant

* FRPC-II: Facilities for Reliability Study of Pressure Boundary Components-II

2. TEST PROCEDURE

2.1 Test Equipment

Figure 2.1 shows the test equipment of cross-over leg pipe whip tests RUNs 5808 and 5809. A heater vessel contains the electric heater of 400 kW, and is used to heat up a pure water in this test loop. High pressurized and high temperature water is stored in a pressure vessel and circulated by a circulating pump. A pressurizer contains the electric heater of 30 kW, and is used to make subcooled water in the pressure vessel. The test pipe for the cross-over leg pipe whip test is attached to the nozzle of the pressure vessel through a connecting pipe.

Figures 2.2 to 2.4 show the assemblage of test equipments of the connecting pipe, the test pipe and the pipe support. The connecting pipe was made of 8-inch schedule 160 pipe, and was bent to absorb the thermal expansion of the piping. The rod supports were placed for the connecting pipe not to move by the water hammer just after the break. A pipe support was placed at the connecting point between the connecting pipe and the test pipe, and fixed the displacements in the X, Y and Z directions. Table 2.1 summarizes the name of each equipment. Photograph 2.1 shows the above view of the test equipments before the test.

Figures 2.5 and 2.6 show the detail assemblages of the test pipe and the restraints. The test pipe was fabricated from 6-inch schedule 120 pipe (inner diameter = 136.6 mm, thickness = 14.3 mm), made of type 304 stainless steel whose chemical composition and mechanical properties were shown in Table 2.2. Table 2.3 shows the chemical composition and mechanical properties of the restraints made of carbon steel. A rupture disk was jointed to the free end of the pipe by using a graylock flange. Figure 2.7 shows the details of the rupture disk. The water in the pipe was discharged by breaking the rupture disk using the electric arc method. Photographs 2.2(a)(b) show the views of two arc electrodes attached to the rupture disk.

2.2 Test Condition

Table 2.4 summarizes the test conditions of RUNs 5808 and 5809.

The test of RUN 5808 was performed to measure the thermal expansion of piping when the fluid temperature attained 325 °C. Pressure in the loop was 12.05 MPa. The rupture disk was not broken, since the test of RUN 5808 purposed only to measure the thermal expansion of piping. Temperature and pressure in the loop decreased to zero naturally.

Estimating the thermal expansion of piping obtained from the test of RUN 5808, we adjusted the gaps of restraints to become 0.3 mm just before the break of the rupture disk in the test of RUN 5809. Temperature and pressure in the loop were increased to 322.6 °C and 15.3 MPa. Water in the loop was circulated to the pipe end at the test section through a warming up line by using the circulating pipe. Temperature at the test section was 315.0 °C just before the break.

2.3 Measuring Items and Devices

(1) Electrical measurements

Table 2.5 summarizes the electrical measuring items, e.g. strain gages, pressure transducers, thermocouples, displacement meters and accelerometers.

Figure 2.8 shows the locations of high temperature strain gages (XU 111 to XU 126) mounted in the axial direction of the test pipe except for only XU 116.

Figure 2.9 shows the locations of the strain gages (XU 131 to XU 136) attached to the restraint III in the axial direction. As shown in the Fig. 2.9, four couples of bi-axial strain gages were attached to the root of the restraint III to make load transducers (WU 131 and WU 132), which were used to measure the reaction forces of the restraint III.

The load cells (WU 111 to WU 114) were mounted under and beside the restraint I and II to measure the reaction forces of these restraints. Each load cell could measure 50 ton in load.

The pressure transducers, PU 101, PU 103, PU 105 and PU 111 to PU 116, were mounted to the pressure vessel and piping. Among those, the pressure transducers, PU 101, PU 103 and PU 105, were mounted at the ends of cooling pipes whose length were about 30 cm. On the other hand, PU 111 to PU 116 were the pressure transducers of water-cooled type.

The fluid temperatures in the pressure vessel and piping were measured with the C-A sheathed thermocouples, TU 101, TU 102, TU 104

and TU 111 to TU 116.

The strain gage type displacement meters (XU 201 to XU 205) were installed near the three restraints to monitor the pipe movement during heating up as shown in Fig. 2.8.

The piezo-electric accelerometers XU 301 to XU 305 were mounted on the test pipe as shown in Fig. 2.8.

The high temperature strain gages XU 501 to XU 506 were attached to six blades of the rupture disk to measure the opening times of them as shown in Photo. 2.3.

Almost all transducer outputs were recorded on the five analog data-recorders at the speed of 60 in/sec. Those records were able to reproduce at the minimum sampling period of 12.5 microsec. Other transducer outputs were recorded on XY-recorders for monitoring.

(2) Residual deformation measurements

The following residual deformations were obtained from the variation of the distance between two marking points before and after the test.

1) Residual strains of the test pipe: The axial distances between marking points on the surface of the test pipe were measured with slide calipers before and after the test.

2) Residual cross-sectional deformations of the test pipe: The variations of outer diameters before and after the test were measured with outside calipers.

3) Residual deformations of the test pipe: The heights of the test pipe from the base level were measured with a transit before and after the test.

4) Residual deformation of the restraint III: The lengths and the rotations of the restraint III were measured with scales.

2.4 Test Procedure

The test equipments were set as shown in the Fig. 2.1, and the loop was filled with water by a pump, and was pressurized to 150 kg/cm² (14.7 MPa) by an injection pump in order to check no leakage from the flange.

Only outputs from the displacement meters XU 201 to XU 205 were recorded on X-Y recorders during heating up to 325° in the test of RUN

5808. After the loop was cooled to room temperature, the gaps between the bracket and the restraint I or II were measured. Table 2.6 summarizes the displacements of five meters due to thermal expansion of piping at temperature 325 °C. From these results, we determined the thickness of a shim between the restraints and the bracket for the gaps to be 0.3 mm just before the break of the rupture disk in the test of RUN 5809. Table 2.7 summarizes the thicknesses of shims, and the gaps between the shim and the bracket. The shims were made of a plate steel, and welded at five points of the restraints I, II and III.

Two arc electrodes were attached to the rupture disk in the test of RUN 5809 in order to improve the breaking mode of the rupture disk as shown in Photo. 2.3(a). However, the rupture disk did not fully open at the test, and remained with three blades among six as shown in Photo. 2.3(b). Even the two arc electrodes could not make the rupture disk fully open. Therefore, it seems that the blowdown force of this test was less than that of other tests using 6-inch pipe under the PWR LOCA conditions.

Table 2.1 Name of each equipment

No.	Name
①	Test Pipe
②	Connecting Pipe
③	Pipe Support
④	Support A for Connecting Pipe
⑤	Support B for Connecting Pipe
⑥	Support C for Connecting Pipe
⑦	Support D for Connecting Pipe
⑧	Restraint I and II
⑨	Restraint III

Table 2.2 Chemical composition and mechanical properties of test pipe
(type 316)

Chemical Composition

ELEMENT	C	Si	Mn	P	S	Ni	Cr	Mo
RESULT (%)	0.04	0.52	1.52	0.025	0.004	12.85	16.40	2.11

Mechanical Properties

ITEM	Yield Strength (MPa)	Tensile Strength (MPa)	Elongation (%)
RESULT(%)	294	568	64.0

Table 2.3 Chemical composition and mechanical properties of restraint
(carbon steel)

Chemical Composition

ELEMENT	C	Si	Mn	P	S
RESULT (%)	0.17	0.34	1.35	0.017	0.003

Mechanical Properties

ITEM	Yield Strength (MPa)	Tensile Strength (MPa)	Elongation (%)
RESULT (%)	363	539	30.0

Table 2.4 Test conditions

RUN No.		5808	5809
Test Date		'84, Feb. 21	'84, Apl. 17
Pressure		12.05 MPa	15.28 MPa
Temperature	Pressure Vessel	325.9 °C	322.6 °C
	Test Section	320.7 °C	315.0 °C
Inner Diameter (I. D.) & Thickness(t) of Test Pipe		I. D. = 136.6 mm t = 14.3 mm	

Table 2.5 Measuring items

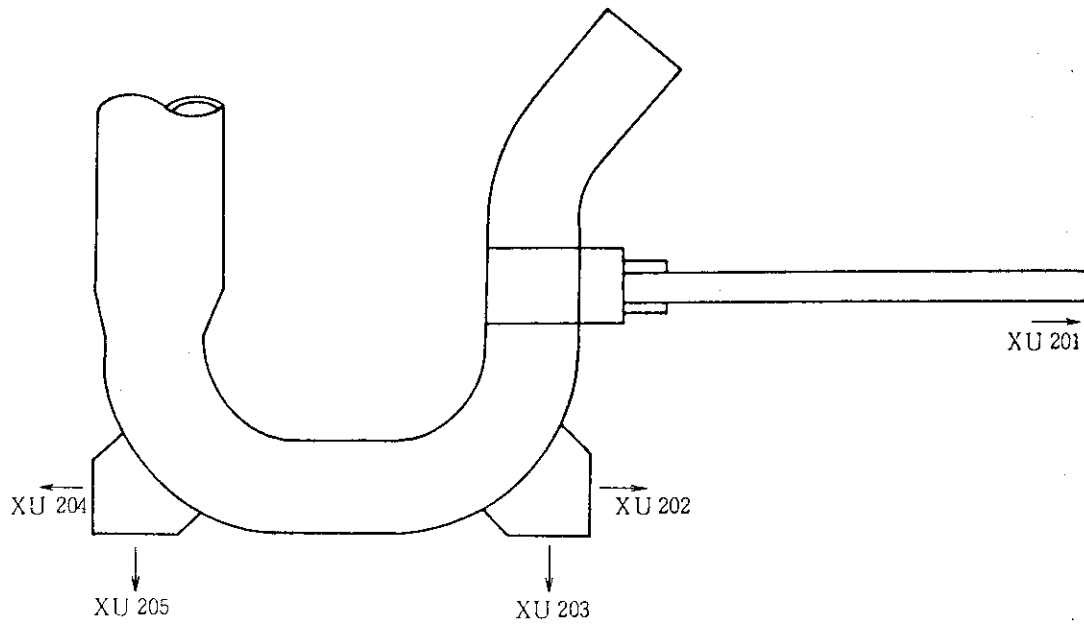
TAG No.	LOCATION	SPECIFICATION	MANUFACTURER TYPE	RECORD DEVICE	
STRAIN GAGE - PIPE					
XU 111	See Fig. 2. 8	High Temp Spot Welded Plastic Strain Gage	AILTECH SG-125-01F (4) -4-SUS 304	<div>M ↑ ↓ M</div>	A 1
112					2
113					3
114					4
115					5
116					6
117					7
118					8
119					9
120					10
121					11
122					12
123					13
124					B 1
125					2
126					3
STRAIN GAGE-RESTRAINT					
XU 131	See Fig. 2. 9	Plastic Strain Gage	TOKYO SOKKI YL-5	<div>M ↑ ↓ M</div>	C 1
132					2
133					3
134					4
135					5
136					6
RESTRAINT FORCE TRANSDUCER					
WU 131	See Fig. 2. 9 & Fig. 2. 3	Elastic	KYOWA	<div>M ↑ ↓ M</div>	C 7
132			KFD-2-D16-11		8
111			TOKYO SOKKI KZ 50 TF		9
112					10
113					11
114					12
PRESSURE					
PU 101	See Fig. 2. 3	Strain Gage Type	BLH	<div>M ↑ ↓ M</div>	C 13
103			GP-200H		B 4
105			SHINKOH MP-200		5
111					6
112					7
113					8
114					9
115					10
116					11

Table 2.5 (Continued)

TAG No.	LOCATION	SPECIFICATION	MANUFACTURER TYPE	RECORD DEVICE	
TEMPERATURE					
TU 101	See Fig. 2.3	C-A, 0.5 ϕ	OKAZAKI	B	B12
102				↑	13
104					D 1
111		C-A, 0.3 ϕ	SUKEGAWA		2
112					3
113					4
114					5
115				↓	6
116		B	7		
DISPLACEMENT					
XU 201	See Fig. 2.8	Strain Gage Type	KYOWA CDP-50	L	XY
202				↑	
203					
204				↓	
205				L	XY
ACCELERATION					
XU 301	See Fig. 2.8	Piezoelectric Type	ENDEVCO 2273A	C	E 1
302				↑	2
303					3
304				↓	4
305				C	5
RUPTURE DISK OPENING GAGE					
XU 501	See Fig. 2.10	High Temp Plastic Strain Gage	AILTECH SG-125-01F(4) -4-SUS 304	H	E 6
502				↑	7
503					8
504					9
505					10
506				↓	11
WATER LEVEL					
PD 200	See Fig. 2.1	Water Level	FUJI FEC34WD3		E12
WU 101		Load Cell	BLH T2G-1	L	13

H : High Freq. Amp. (50 kHz) SHINKOH DA- 4007 - F
 M : Medium Freq. Amp. (10 kHz) ... SHINKOH DA- 4006 - F
 B : DC Amp. BLH BLH-5300
 C : Charge Amp. ENDEVCO MODEL 2735
 A 1 }
 { Analog Data Recorder AMPEX PR- 2200
 E13 }
 XY : XY Recorder

Table 2.6 Displacement of five meters by thermal expansion at temperature 325 °C

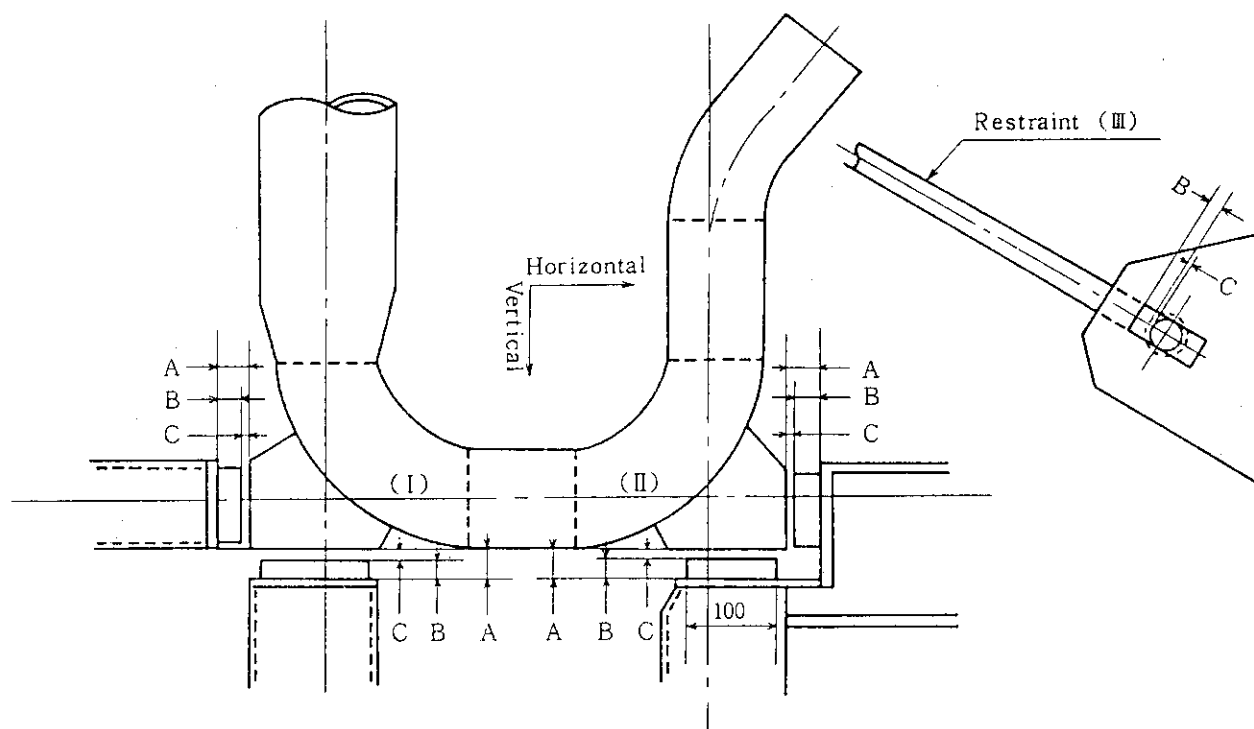


Location	Displacement
X U 201	3.70 mm
X U 202	4.15 mm
X U 203	2.55 mm
X U 204	0.45 mm
X U 205	2.62 mm

Temp. = 325°C

Press. = 122kg/cm² G

Table 2.7 Gaps of three restraints



mm

	Horizontal			Vertical		
	A	B	C	A	B	C
Restraint (I)	9.00	8.25	0.75	8.80	12.20	2.80
Restraint (II)	16.65	5.95	4.48	S 18.20 N 17.80	S 15.38 N 14.88	2.92
Restraint (III)		9.00	0.00			

A : Gap between restraint and bracket

B : Thickness of shim

C : Gap between shim and bracket

S : South side

N : North side

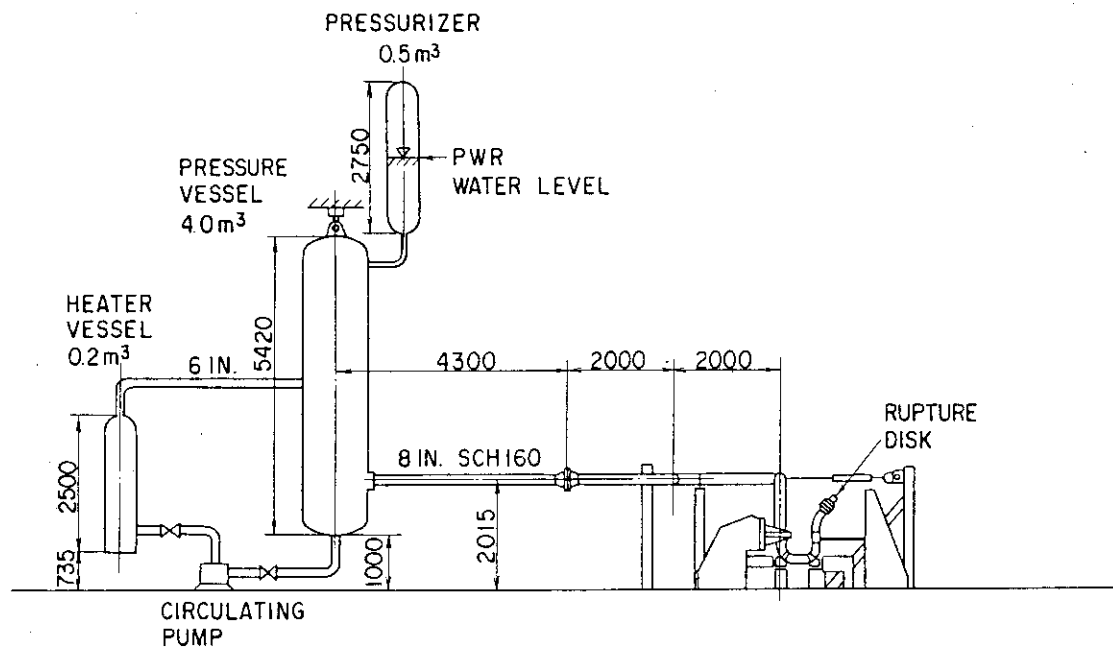


Fig. 2.1 Conceptual figure of the test facilities

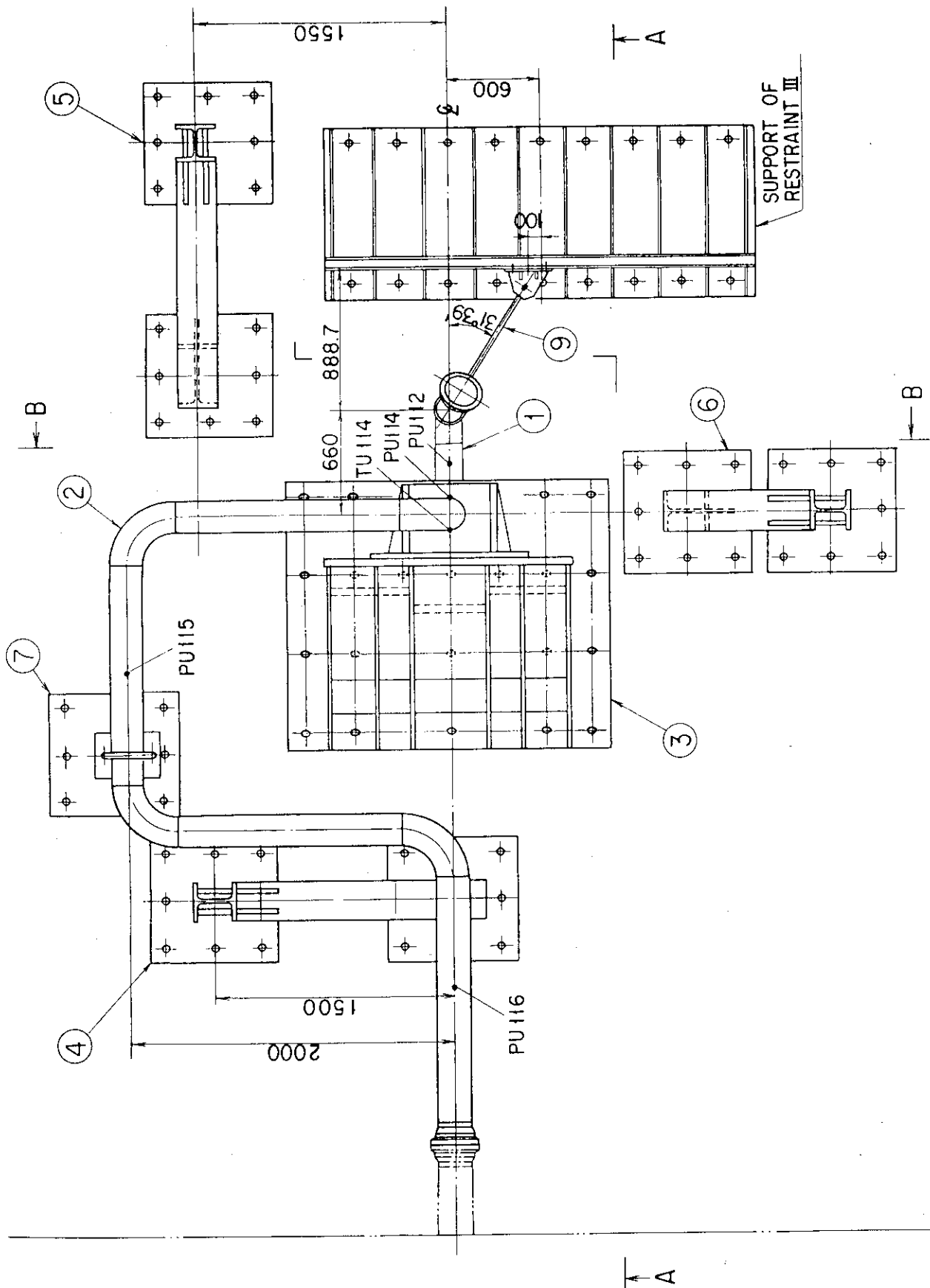


Fig. 2.2 Assemblage of the test equipments (above view)

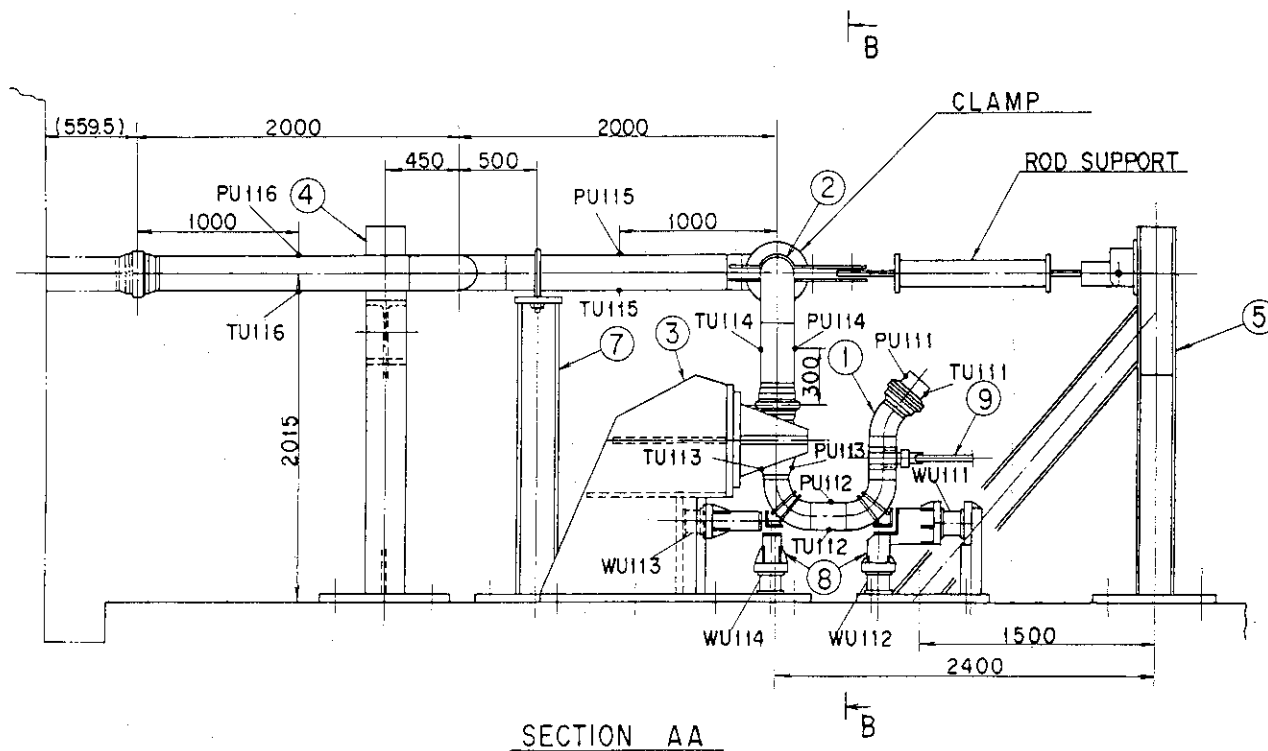


Fig. 2.3 Assemblage of the test equipments (side view)

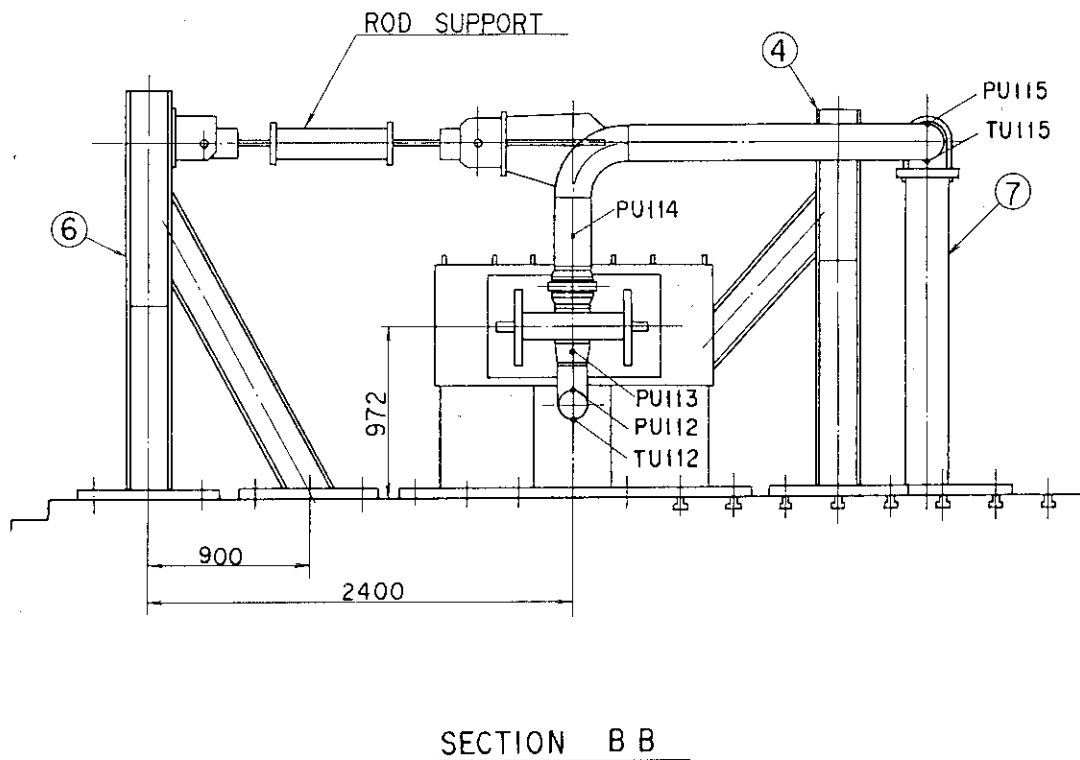


Fig. 2.4 Assemblage of the test equipments (front view)

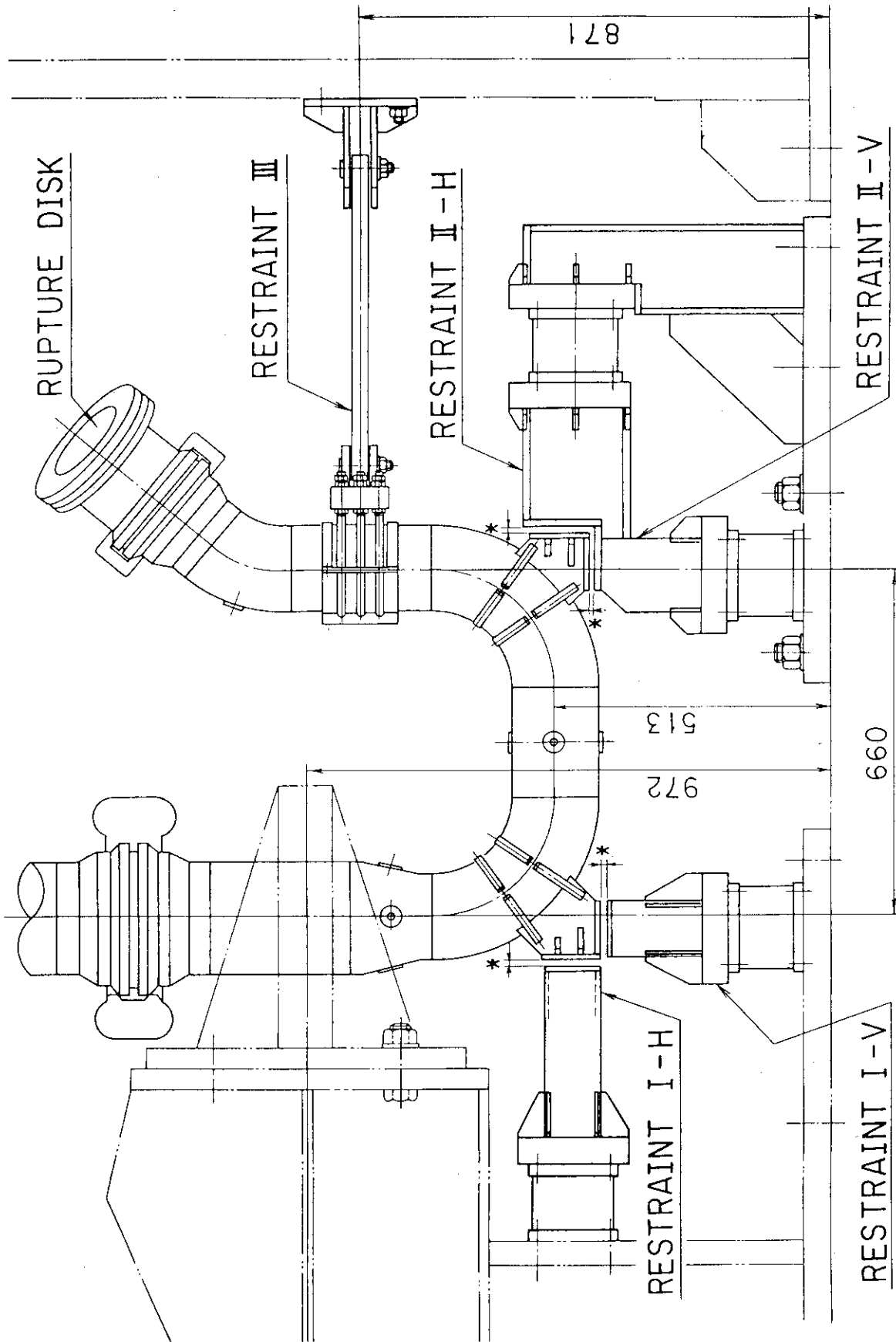


Fig. 2.5 Detail assemblage of the test pipe and the restraints
(side view)

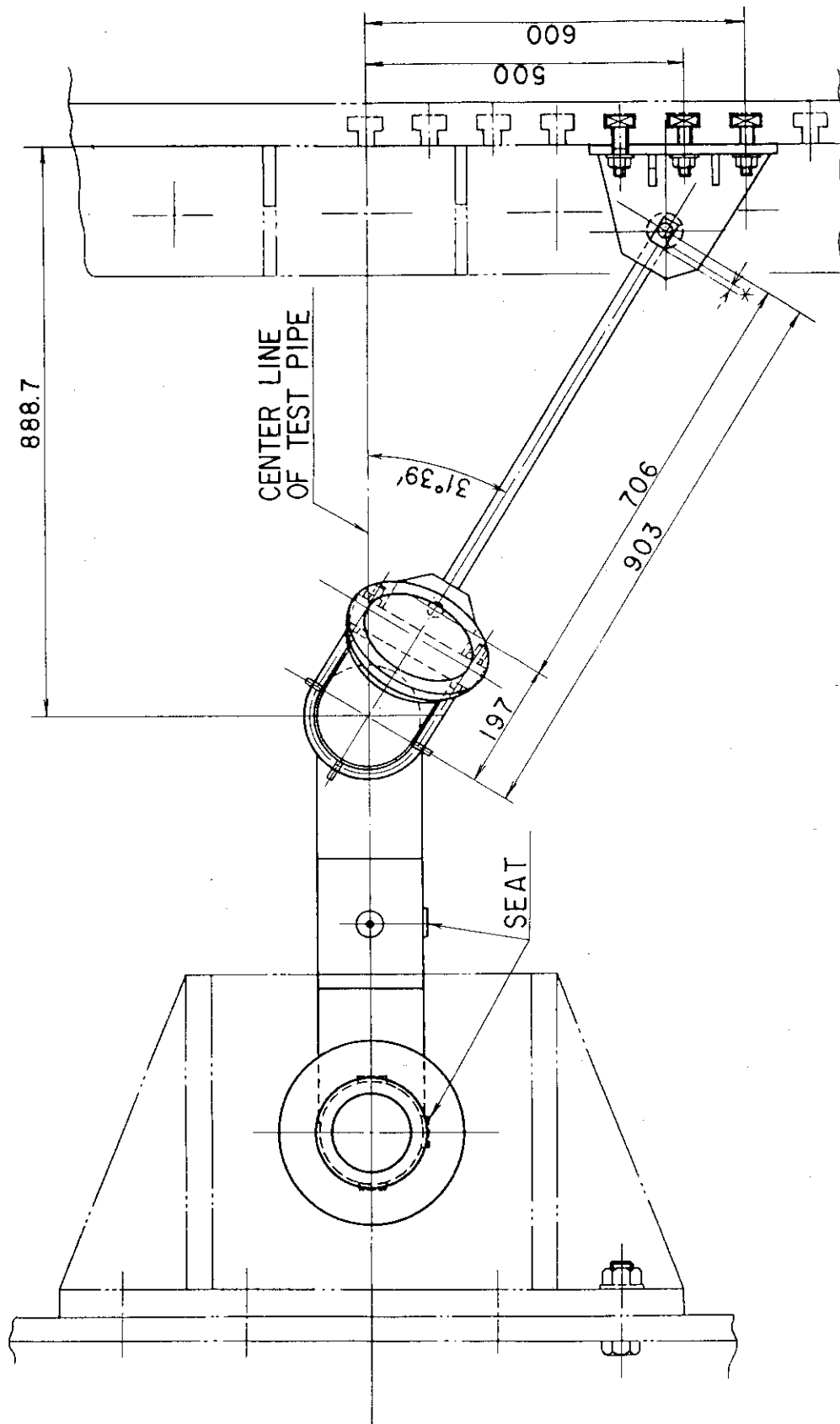


Fig. 2.6 Detail assemblage of the test pipe and the restraints
(above view)

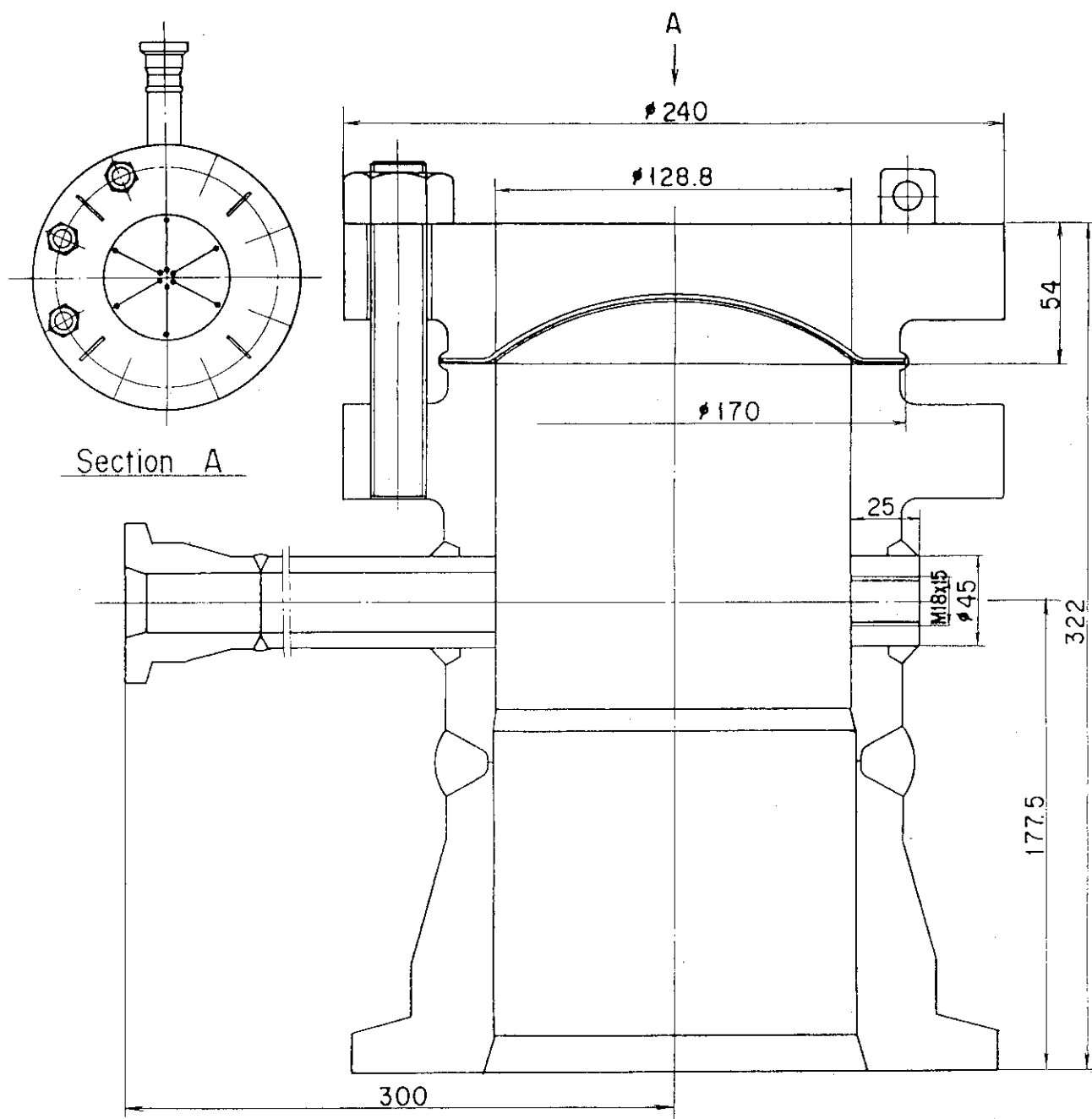


Fig. 2.7 Details of welded rupture disk

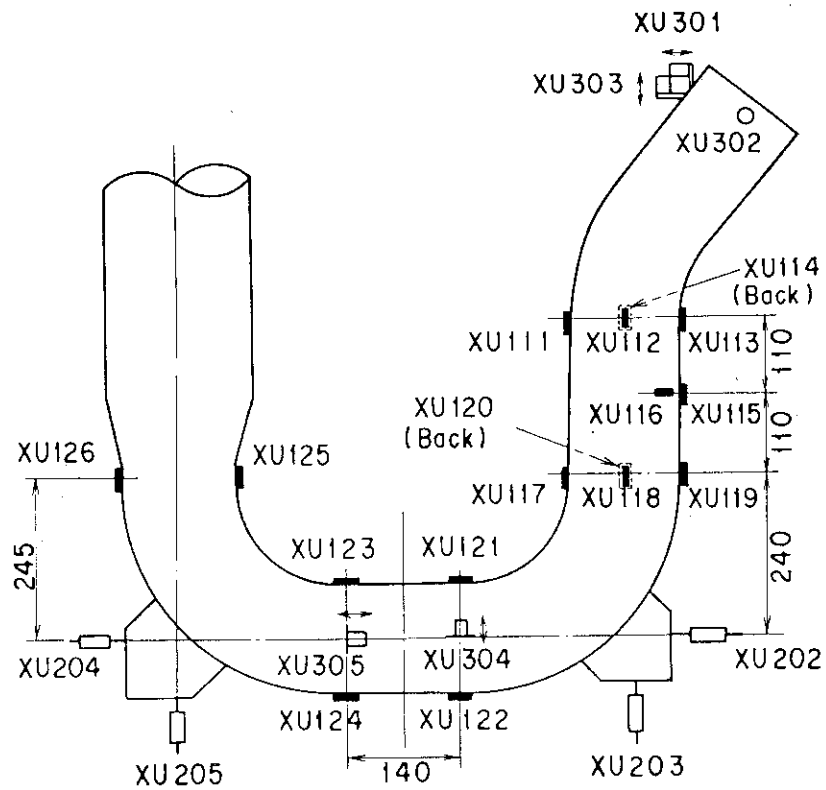


Fig. 2.8 Locations of strain gages mounted on the test pipe

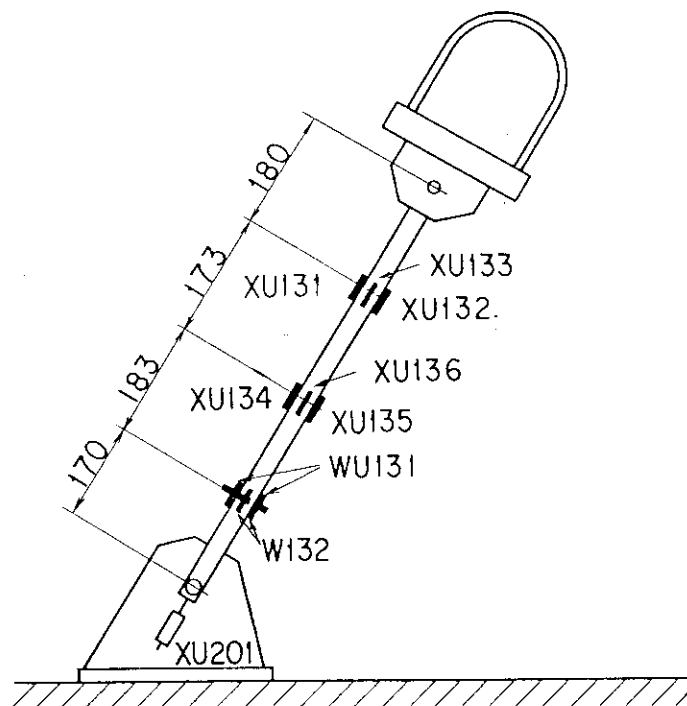


Fig. 2.9 Locations of strain gages mounted on the restraint III

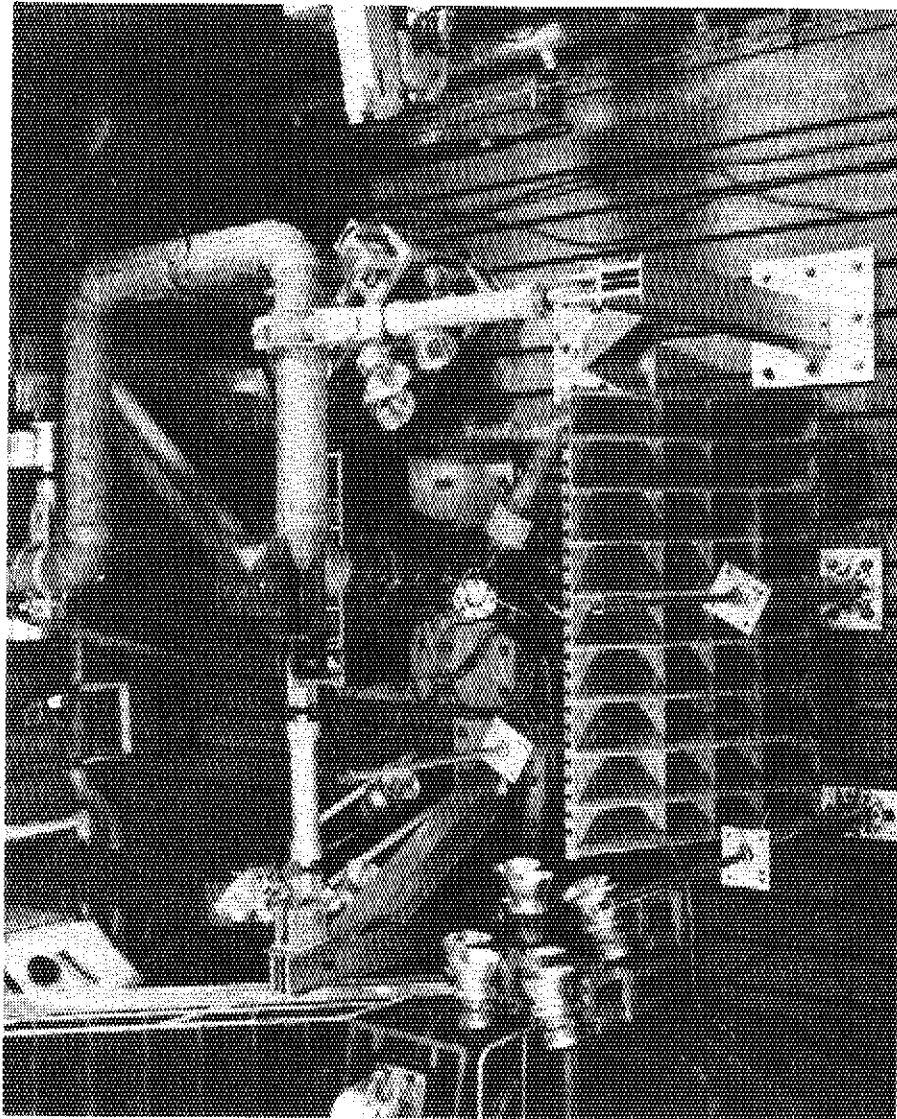
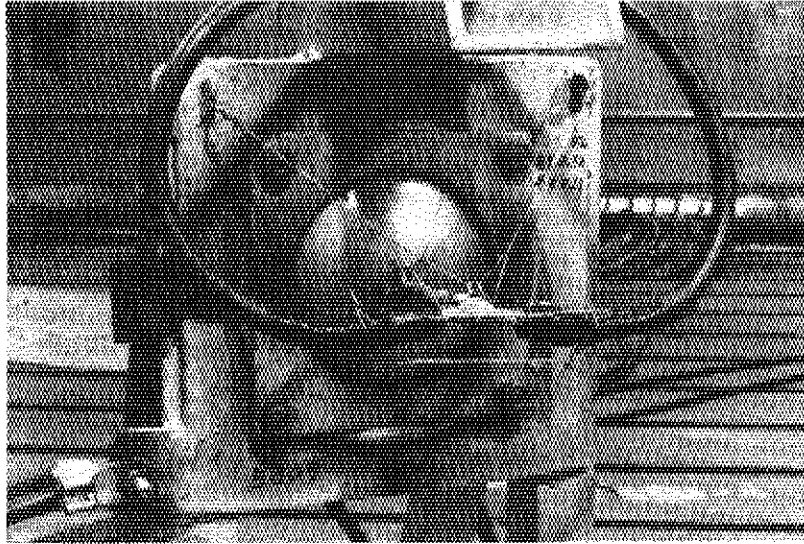
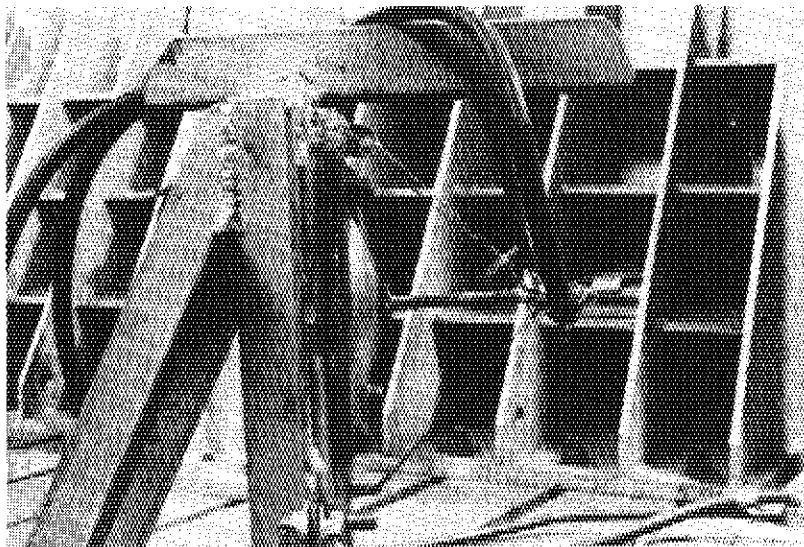


Photo. 2.1 Above view of the test equipments before the test

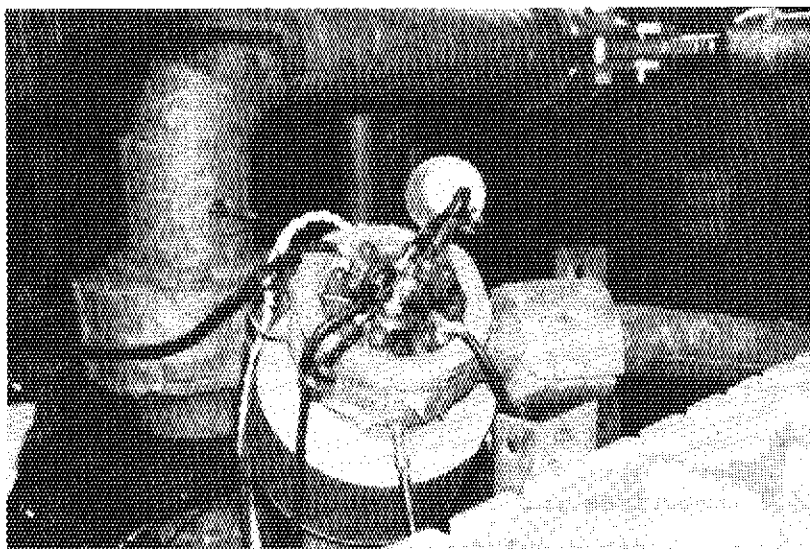


(a) Front View

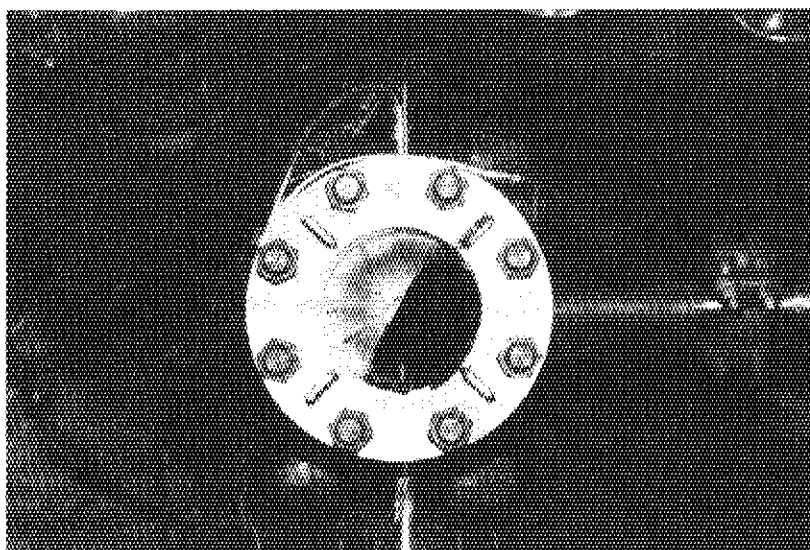


(b) Side View

Photo. 2.2 Views of two arc electrodes attached to the rupture disk



(a) Before Test



(b) After Test

Photo. 2.3 Views of the rupture disk before and after the test

3. TEST RESULTS

3.1 Results of Residual Deformation Measurements

(1) Residual strains of the test pipe

Table 3.1 summarizes the measuring results of the axial distances between markings on the surface of the test pipe. These results show that the straight pipe is almost within elastic deformation, since the residual strains of the test pipe is almost zero.

(2) Residual cross-sectional deformations of the test pipe

Table 3.2 summarizes the measuring results of the outer diameters of the test pipe. These results show that the rate of the residual cross-sectional deformations of the test pipe is less than 0.1 %.

(3) Residual deformations of the test pipe

Table 3.3 summarizes the measuring results of the heights of the test pipe from the base level. These results show that the maximum residual deformation is about 7 mm at the free end of the test pipe.

(4) Residual deformations of the restraint III

Table 3.4 summarizes the measuring results of the residual deformation and rotation of the restraint III. These results show that the elongation of a U-bar is larger than that of a rod.

3.2 Photographs before and after the Test

Photographs before and after the test RUN 5809 are shown in Photo. 3.1(a)(b), Photo. 3.2(a)(b) and Photo. 3.3(a)(b). These photographs show that the test pipe and the restraints do not deform largely after the test. Then it is concluded that the restraints limit the movement of the test pipe effectively.

Photographs 3.4(a)(b) show the attaching locations of the displacement meters XU 201 to XU 205 for measuring the thermal expansion of the piping.

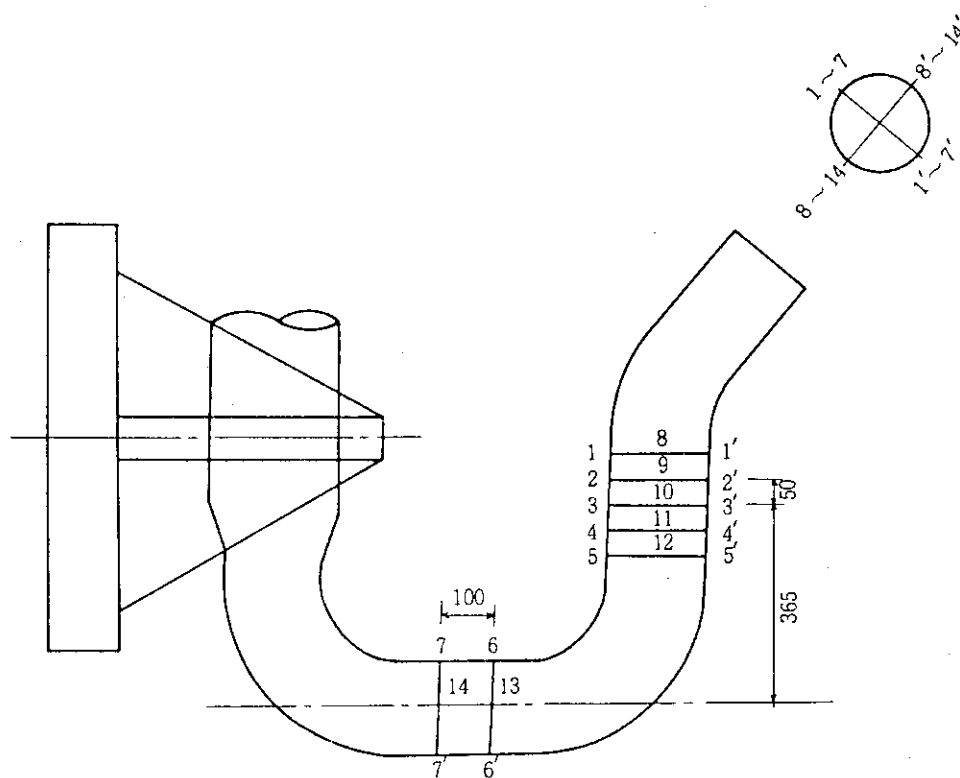
Photographs 3.5(a)(b) show the near views of the restraint I and II after the test RUN 5809. It was observed that the gap between the shim and the bracket remained a little.

Photographs 3.6(a)(b) show the side and above views of the restraint III after the test.

3.3 Observation of Pipe Whip Movement by High Speed Camera

Photograph 3.7 shows the selected frames of a high speed camera. These frames were taken at the speed of 3000 frames/sec.

Table 3.1 Results of dimensional measurements of test pipe

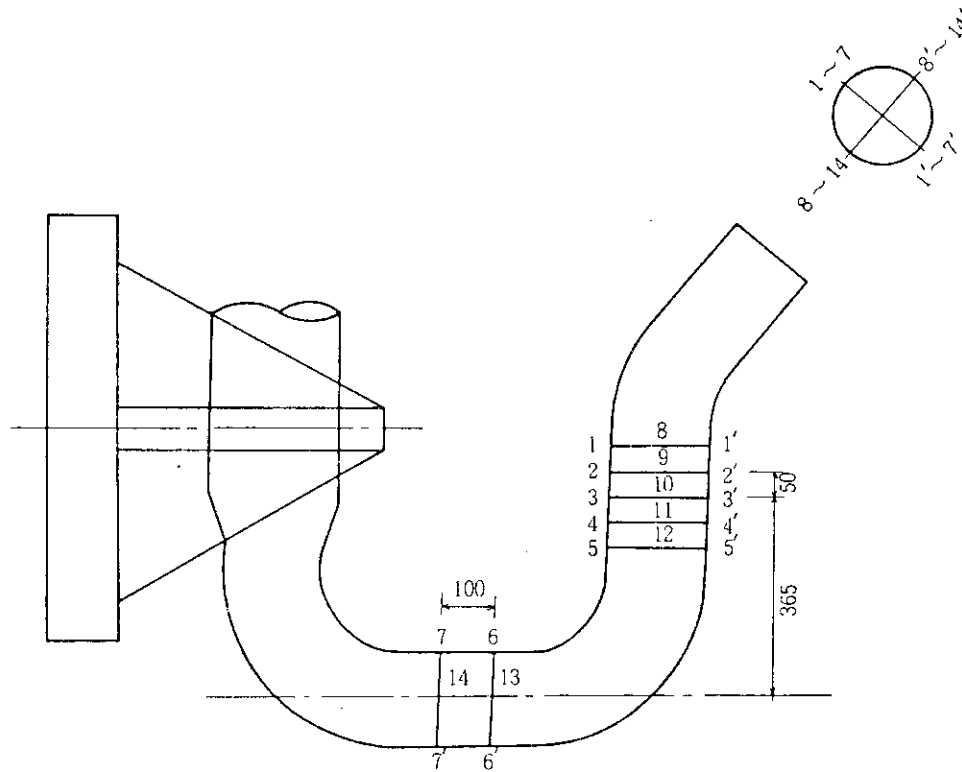


(mm)

	1—2	2—3	3—4	4—5	6—7	1'—2'	2'—3'	3'—4'	4'—5'	6'—7'
Before Test	49.65	49.70	50.00	50.05	100.00	49.80	50.00	49.80	49.65	100.00
After Test	49.65	49.70	50.00	50.05	99.90	49.80	50.00	49.80	49.65	100.10
Difference	0.00	0.00	0.00	0.00	0.10	0.00	0.00	0.00	0.00	0.10

	8—9	9—10	10—11	11—12	13—14	8'—9'	9'—10'	10'—11'	11'—12'	13'—14'
Before Test	49.70	49.70	49.80	49.90	100.25	49.90	49.90	49.80	49.80	99.80
After Test	49.70	49.70	49.80	49.90	100.35	49.90	49.85	49.75	49.75	99.75
Difference	0.00	0.00	0.00	0.00	0.10	0.00	—0.05	—0.05	—0.05	—0.05

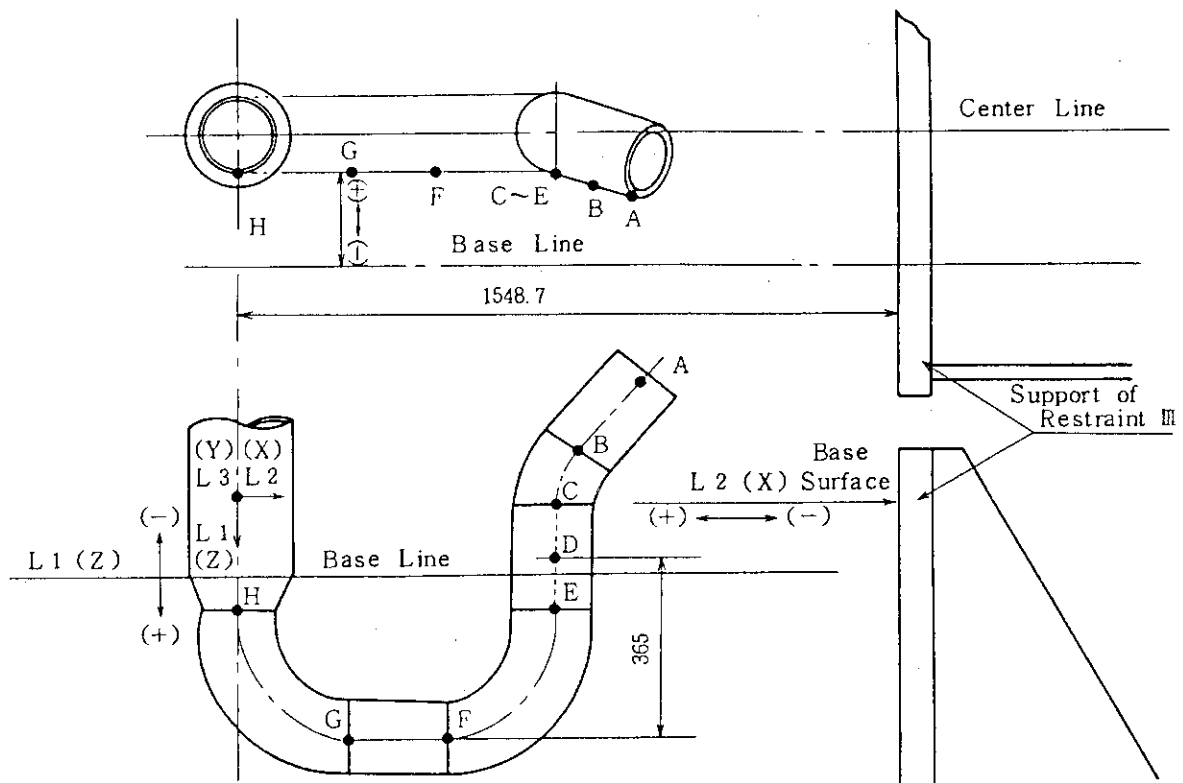
Table 3.2 Results of residual cross-sectional deformation of the test pipe



	(mm)						
	1 - 1'	2 - 2'	3 - 3'	4 - 4'	5 - 5'	6 - 6'	7 - 7'
Before Test	165.05	165.09	165.11	165.15	165.01	164.63	164.99
After Test	165.05	165.16	165.18	165.19	165.06	164.71	165.03
Difference	0.09	0.07	0.07	0.04	0.05	0.08	0.04

	8 - 8'	9 - 9'	10 - 10'	11 - 11'	12 - 12'	13 - 13'	14 - 14'
Before Test	164.68	165.19	165.17	165.12	164.69	165.21	164.98
After Test	164.76	165.20	165.19	165.16	164.77	165.18	164.98
Difference	0.08	0.01	0.02	0.04	0.08	- 0.03	0.10

Table 3.3 Results of residual deformation of the test pipe



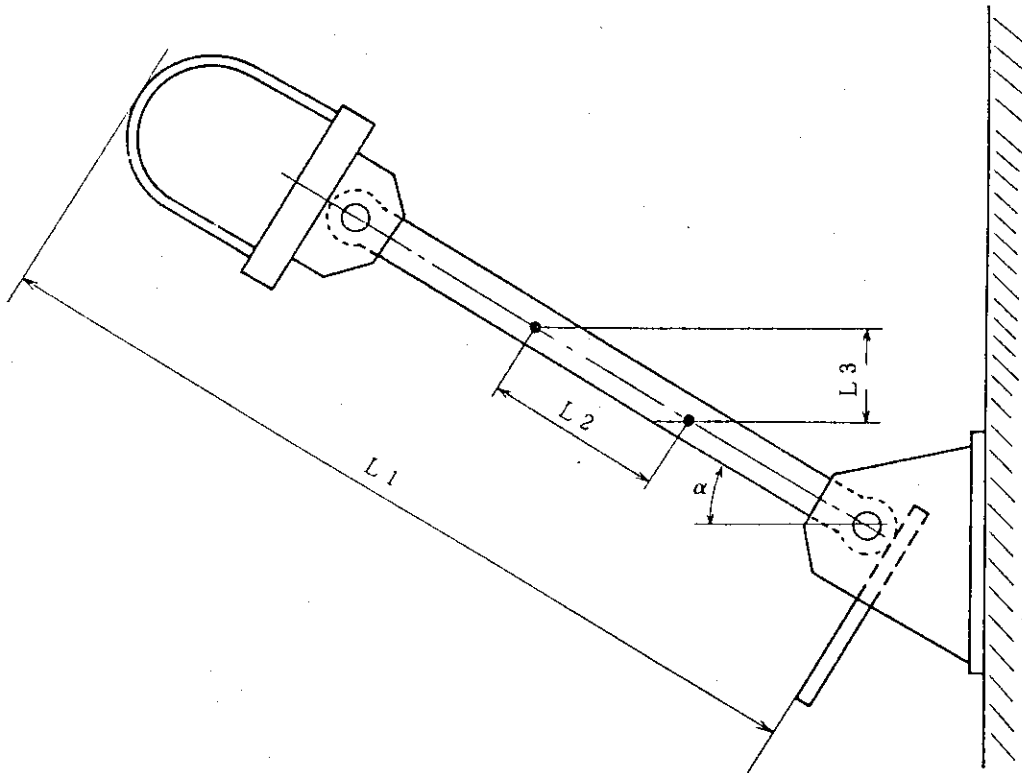
(mm)

		A	B	C	D	E	F	G	H
L 1 (Z)	Before Test	+ 760.0	+ 411.0	+ 252.0	+ 116.0	- 20.5	- 247.5	- 246.5	- 17.0
	After Test	+ 759.0	+ 409.8	+ 251.4	+ 114.7	- 21.0	- 248.3	- 246.8	- 16.8
	Difference	+ 1.0	+ 1.2	+ 0.6	+ 1.3	- 0.5	- 0.8	- 0.3	- 0.2

		A	B	C	D	E	F	G	H
L 2 (X)	Before Test	672.5	882.5	889.5	887.5	887.0	1113.5	1317.5	1541.8
	After Test	671.0	882.0	887.5	887.0	886.5	1113.2	1317.0	1541.5
	Difference	- 1.5	- 0.5	- 2.0	- 0.5	- 0.5	- 0.2	- 0.5	- 0.3

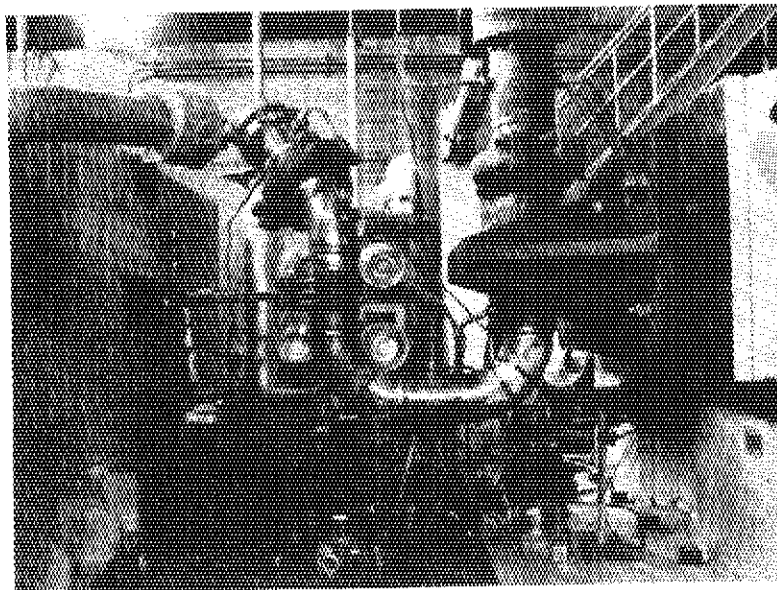
		A	B	C	D	E	F	G	H
L 3 (Y)	Before Test	293.0	467.5	486.0	488.5	487.5	489.5	490.0	487.0
	After Test	299.5	471.5	491.0	491.2	490.0	491.0	491.0	488.0
	Difference	+ 6.5	+ 4.0	+ 5.0	+ 2.7	+ 2.5	+ 1.5	+ 1.0	+ 1.0

Table 3.4 Results of residual deformation of the restraint III

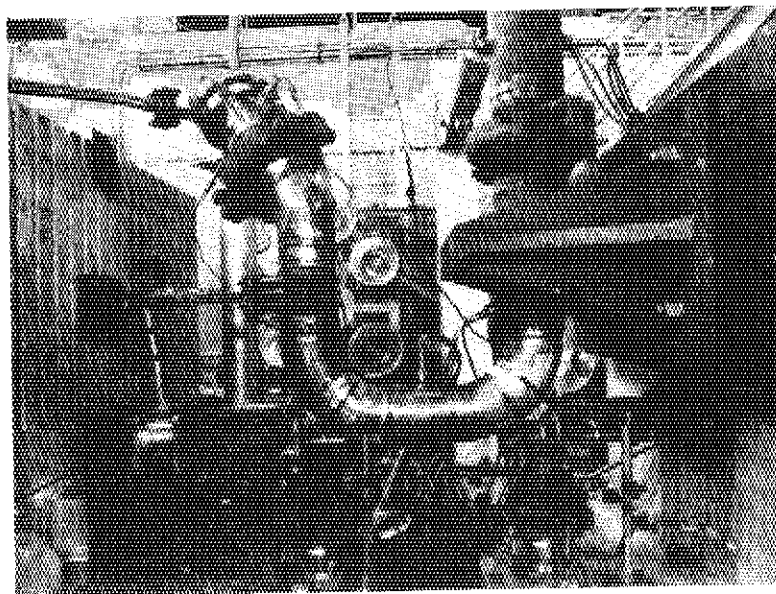


(mm)

	L 1	L 2	L 3	α
Before Test	1022.0	230.0	120.5	31.58°
After Test	1027.5	230.0	121.0	31.73°
Difference	5.5	0.0	0.5	0.15°

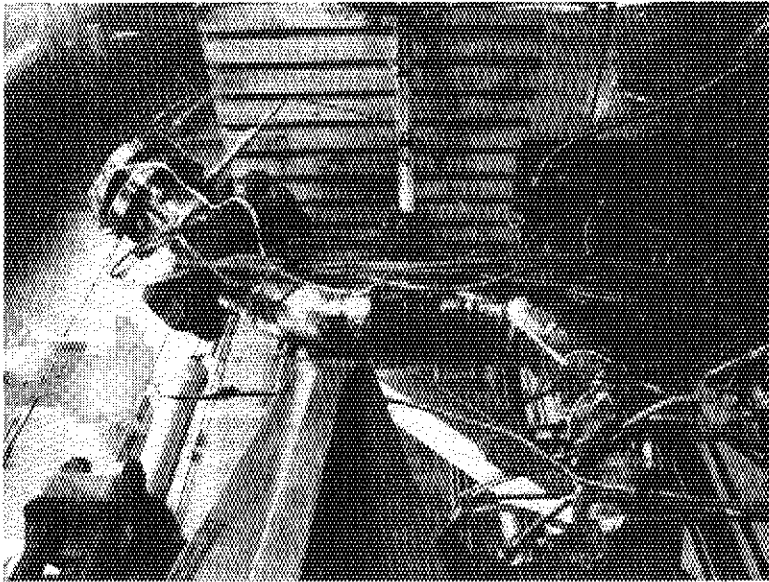


(a) Before Test

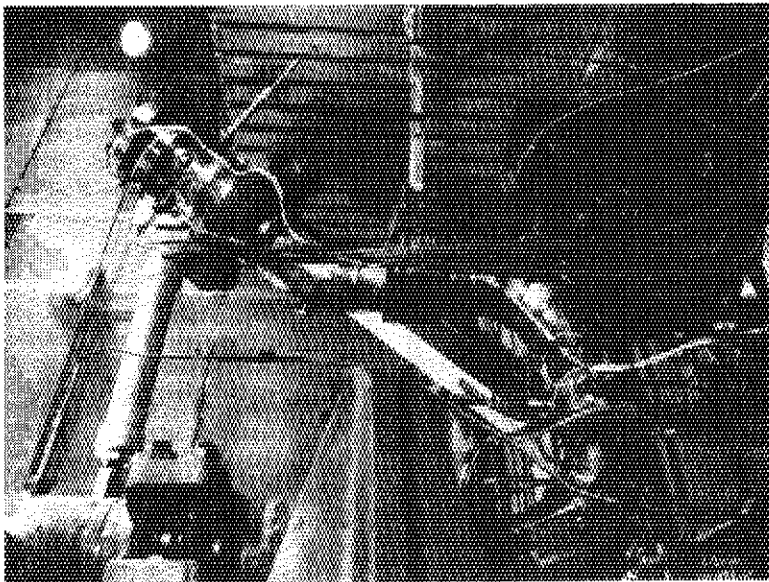


(b) After Test

Photo. 3.1 Side views of the test pipe before and after the test

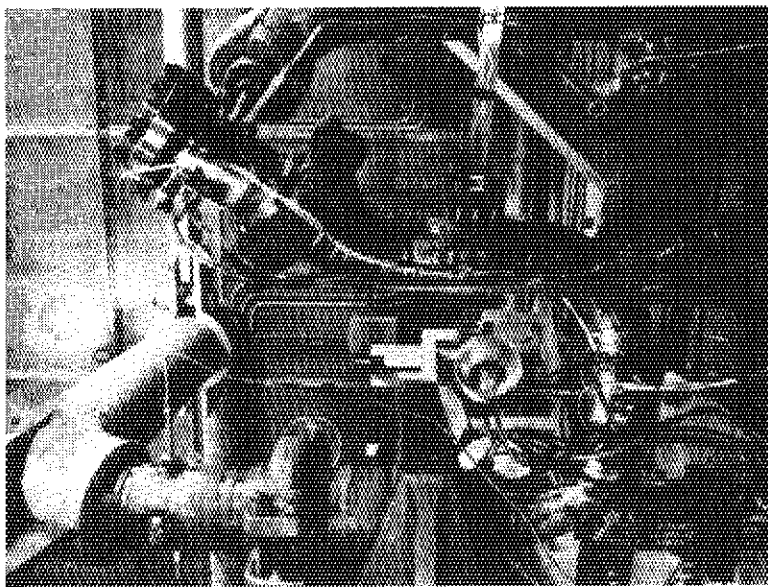


(b) After Test

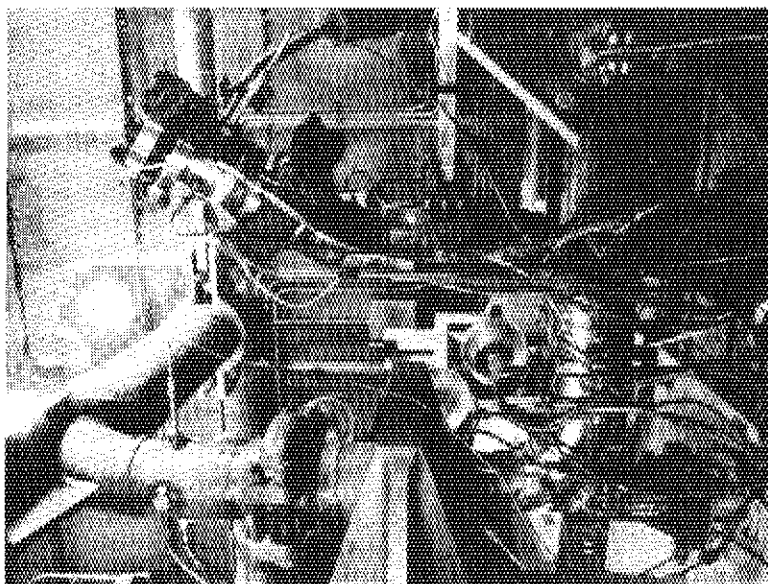


(a) Before Test

Photo. 3.2 Back views of the test pipe before and after the test

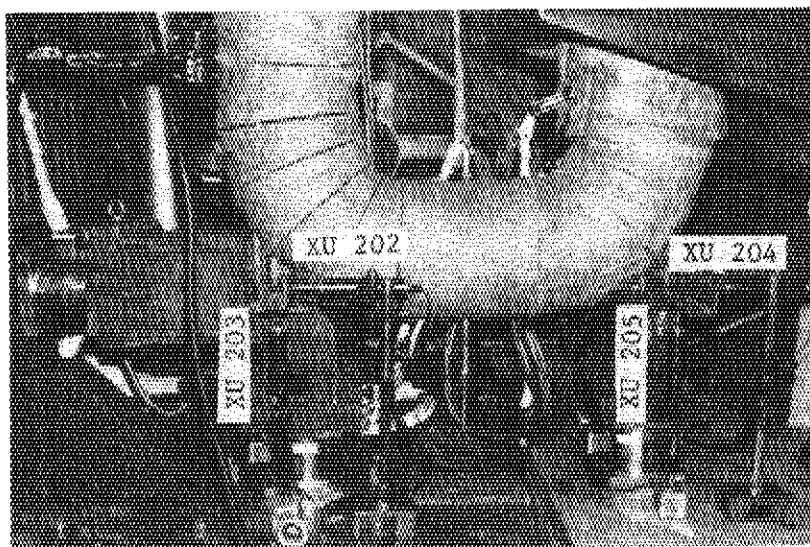


(a) Before Test

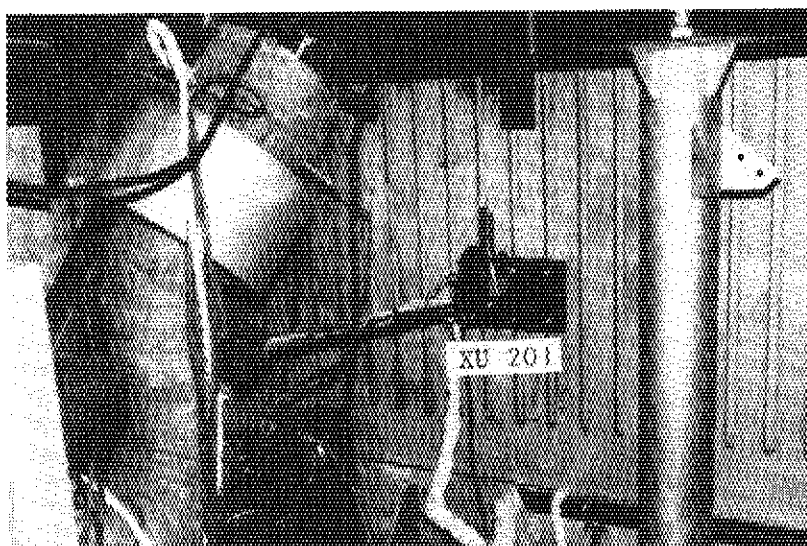


(b) After Test

Photo. 3.3 Another side views of the test pipe before and after the test

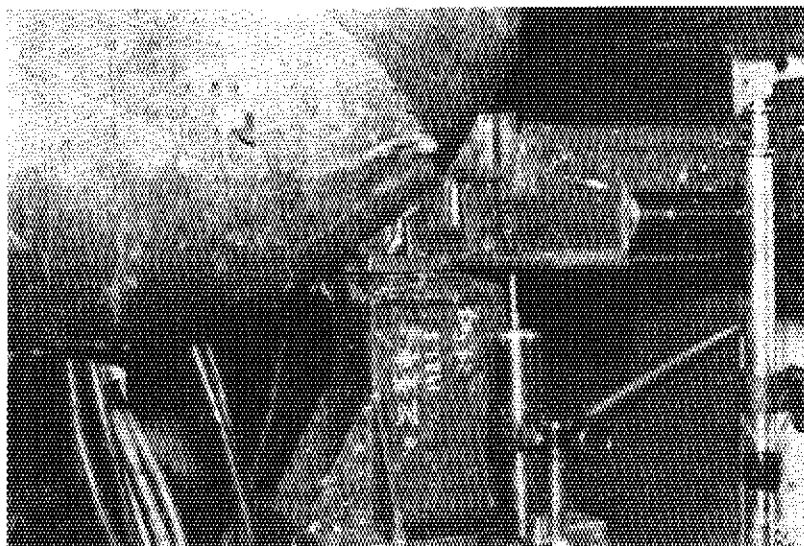


(a) XU 202 ~ XU 205

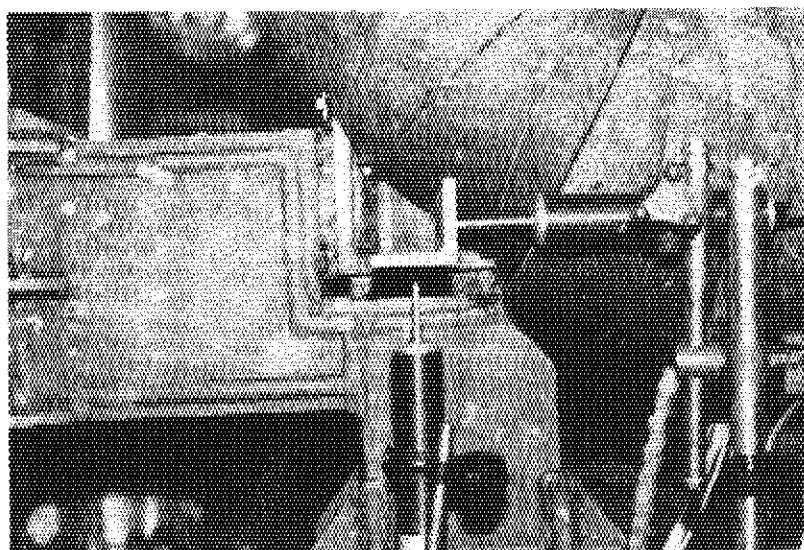


(b) XU 201

Photo. 3.4 Five displacement meters

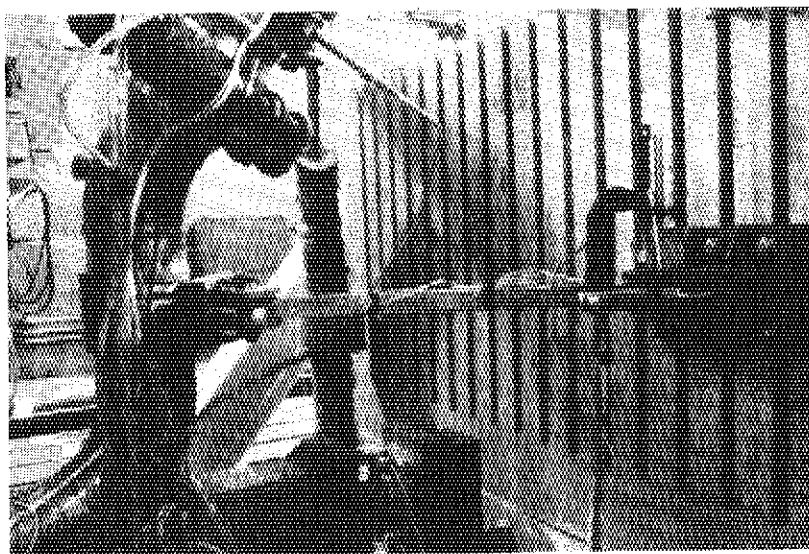


(a) Restraint I

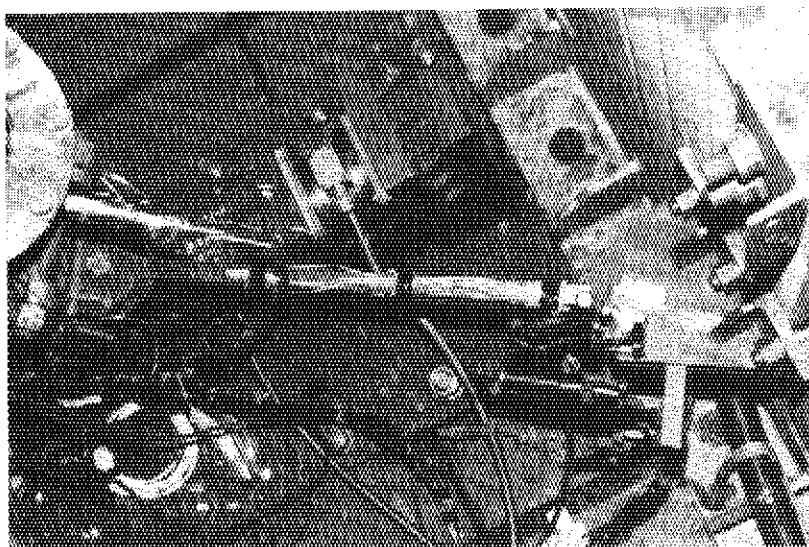


(b) Restraint II

Photo. 3.5 Near views of the restraints I and II after the test



(a) Side View



(b) Above View

Photo. 3.6 Side and above views of the restraint III after the test

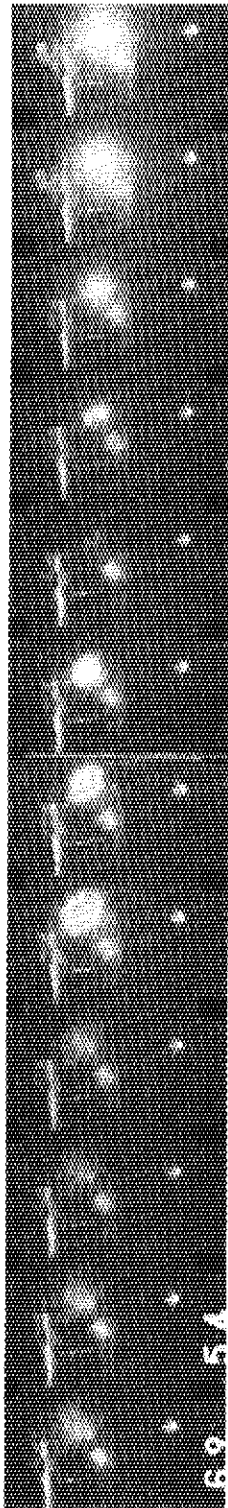


Photo. 3.7 Selected frames of the high speed camera (3000 frames/sec)

4. DISCUSSION

4.1 Time Sequence of the Major Events

Almost all transducer outputs were amplified and recorded on the five analog data-recorders at the speed of 60 in/sec. The start time of the data-recorders was set before the pipe whip movement, that is, at the time when a current began to flow into a electrode for breaking the rupture disk. The time sequence of the major events is shown in Fig. 4.1, where each tag number denotes the first signal from each detector described in the Table 2.5. It took about 56.5 msec from the start of recording the first signal of the accelerometers XU 301, XU 302 and XU 303. Namely, it took about 56.5 msec from beginning of current into the electrode to breaking of the rupture disk. The outputs of XU 301, XU 302 and XU 303 appear the earliest, so that the first beginning time of the pipe whip movement can be defined as the starting time of these outputs.

4.2 Pressure Decrease in the Vessel and the Pipe

The initial conditions of pressure and temperature were already shown in Table 2.4. Pressure histories of PU 103 and PU 111 are shown in Fig. 4.2. These pressures drop rapidly from subcooled state to saturated one just after the break of rupture disk. Then, the pressures decrease in saturated relation with water temperature. The slope of the pressure-time curve changes suddenly during saturated decompression owing to the transition from the low quality discharge to the high quality one.

The comparison of pressure histories along the pipe is shown in Fig. 4.3. These pressures drop in stepwise manner just after the break. This is due to the propagation of the pressure wave i.e. the water hammer, toward the pressure vessel. Velocity of the pressure wave propagating in the fluid becomes about 850 m/sec as shown in Fig. 4.4, and is almost equal to the velocity of sound in the subcooled water at 320 °C temperature and 15.6 MPa pressure.

4.3 Deformation of the Test Pipe

(1) Deformation due to the thermal expansion

As shown in Table 2.6, each part of the test pipe moved a few millimeters by the thermal expansion of piping in RUN 5808 test. Figure 4.5 shows the relation between the thermal expansion of each part and the temperature in the loop. The jointed point between the test pipe and the connecting pipe was fixed in X, Y and Z directions by the pipe support, so that the thermal expansion of the connecting pipe was not transmitted to the test pipe. Therefore, the horizontal thermal expansion at XU 204 near by the restraint I was only about 0.4 mm. The displacement meters XU 203 and XU 205 measured the vertical thermal expansion near by the restraints I and II, respectively, and had almost same expansion-temperature curves. The displacement meter XU 202 measured the horizontal thermal expansion nearby the restraint II, and had the highest expansion-temperature curve among five curves.

(2) Residual deformation

The test pipe after the test RUN 5809 did not have large residual deformation as shown in Photos. 3.1(a)(b) to 3.3(a)(b). Plastic strain of the test pipe was less than 0.1 % as shown in Tables 2.8 and 2.9. Figure 4.6 shows the residual deformation of the test pipe after the test RUN 5809 by using the vector display. The residual deformations in Y direction were larger than those in X and Z directions. All residual deformations were minus values in X direction and in Y direction.

(3) Dynamic deformation

Figure 4.7 shows the maximum strain values of gages attached to the test pipe. The sign before each value, + means tensile strain and - means compression strain. Output of XU 120 was the largest absolute strain value of the sixteen gages attached to the test pipe, and became about - 6 mm at 0.05 sec.

Table 4.1 summarizes the five gaps before and after the break of the rupture disk. Each value in the column (1) is the gap between the shim and the bracket at room temperature as shown in Table 2.7. Each value in the column (2) is the displacement of piping due to the thermal expansion at 325 °C temperature in the test RUN 5809. Each

value in the column (3) in the gap just before break of the rupture disk, and equals to (1) minus (2). Each value in the column (4) is the output value of each displacement meter at 0.5 sec after the break. The pipe at the restraints deformed elastically more than each gap, since each value in the column (4) is a few times as large as that in the column (3).

4.4 Deformation of Restraint

The restraints I, II and III deformed little plastically as shown in Photo. 3.5(a)(b) and Photo. 3.6(a)(b). The rod of the restraint III was within elastic state, since L 2 was 230.0 mm before and after the test as summarized in Table 3.4. On the other hand, the U-bar of the restraint III deformed plastically, since L 1 after the test was longer than that before the test. Angle between the restraint III and the center line increased by 0.15° after the test.

4.5 Acceleration of Test Pipe

Three accelerometers XU 301, XU 302 and XU 303 were attached to the pipe end for detecting the acceleration in X, Y and Z directions, respectively. Two accelerometers XU 304 and XU 305 were attached to the test pipe as shown in Fig. 2.8, and detected the acceleration in Z and X directions, respectively. These accelerometers detected acceleration more than 500 G just after the break. The accelerometer XU 305 detected a little acceleration just after the break, and became zero at about 0.1 sec just after the break.

4.6 Restraint Force

Load histories of WU 131, WU 132, WU 111, WU 112, WU 113 and WU 114 mounted on the restraint I, II and III were shown in Fig. 4.8. Load histories of WU 131 and WU 132 were obtained from the strain gages attached to the rod of the restraint III. Both histories were almost same, and had the maximum load 5 ton just after the break, and became about 1 ton at 0.5 sec after the break.

Load histories of WU 111 and WU 112 were obtained from the horizontal and vertical load cells of the restraint III, and the former became about 3.5 ton and the latter became about 4.5 ton at 0.5 sec

after the break. Load histories of WU 113 and WU 114 were obtained from the horizontal and vertical load cells of the restraint I respectively, and the both became about 0.0 ton at 0.5 sec after the break.

From these results, it was observed that the restraints II and III worked effectively, but the restraint I did not work. This is due to the fact that the restraint I in the real PWR plants is mainly designed to limit the whipping pipe against the double ended guillotine break of the pipe at ⑤ or ⑥ points as shown in Fig. 1.

Table 4.1 Measured gaps before and after the break of rupture disk

Unit : mm

		①	②	③	④
Restraint III	XU 201	0.00	-2.33	2.33	6.00
Restraint II	XU 202	4.48	3.96	0.52	1.50
	XU 203	2.92	2.68	0.24	1.20
Restraint I	XU 204	0.75	0.30	0.45	2.20
	XU 205	2.80	2.70	0.10	0.50

① : Gap at room temperature (see Table 2.7)

② : Displacement of pipe by thermal expansion

③ : ① - ②

④ : Displacement of pipe at 0.5 sec after break.

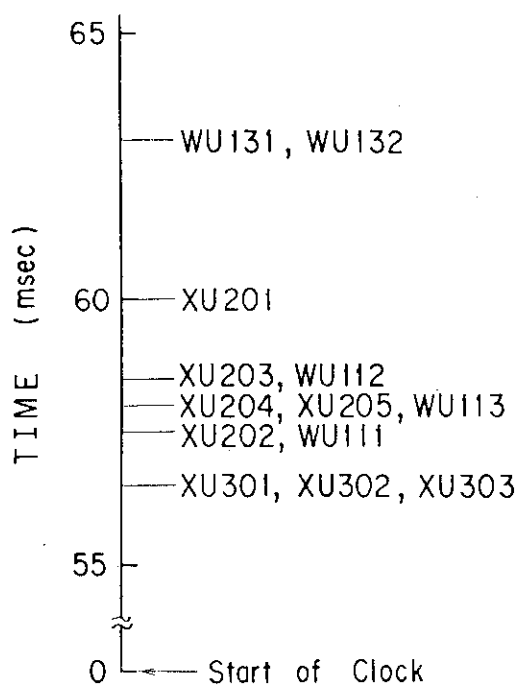


Fig. 4.1 Time sequence of major events

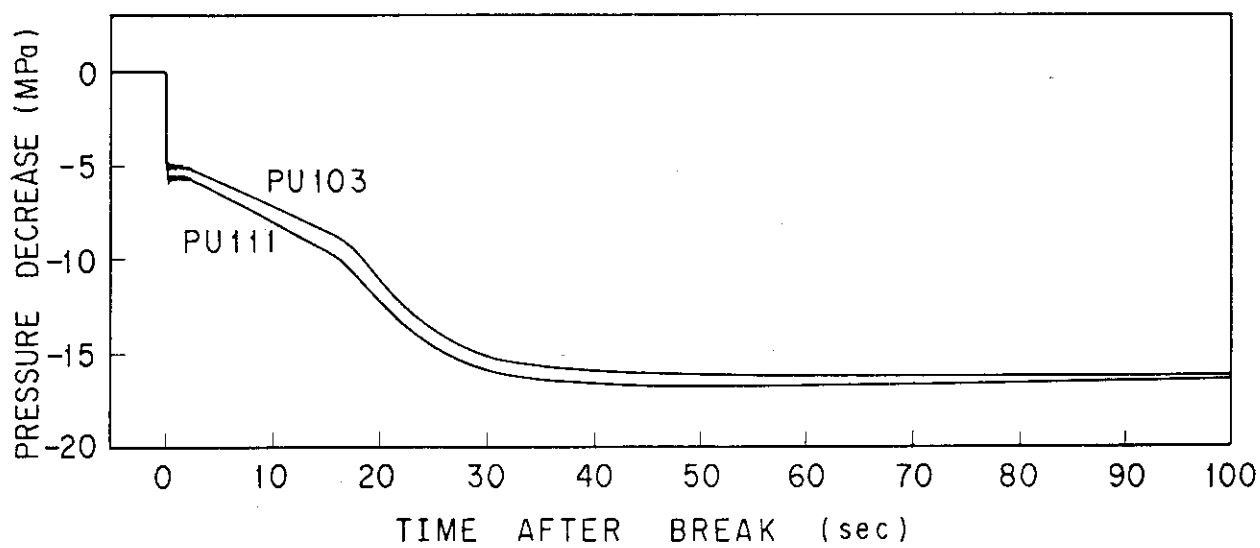


Fig. 4.2 Pressure vs. time curves

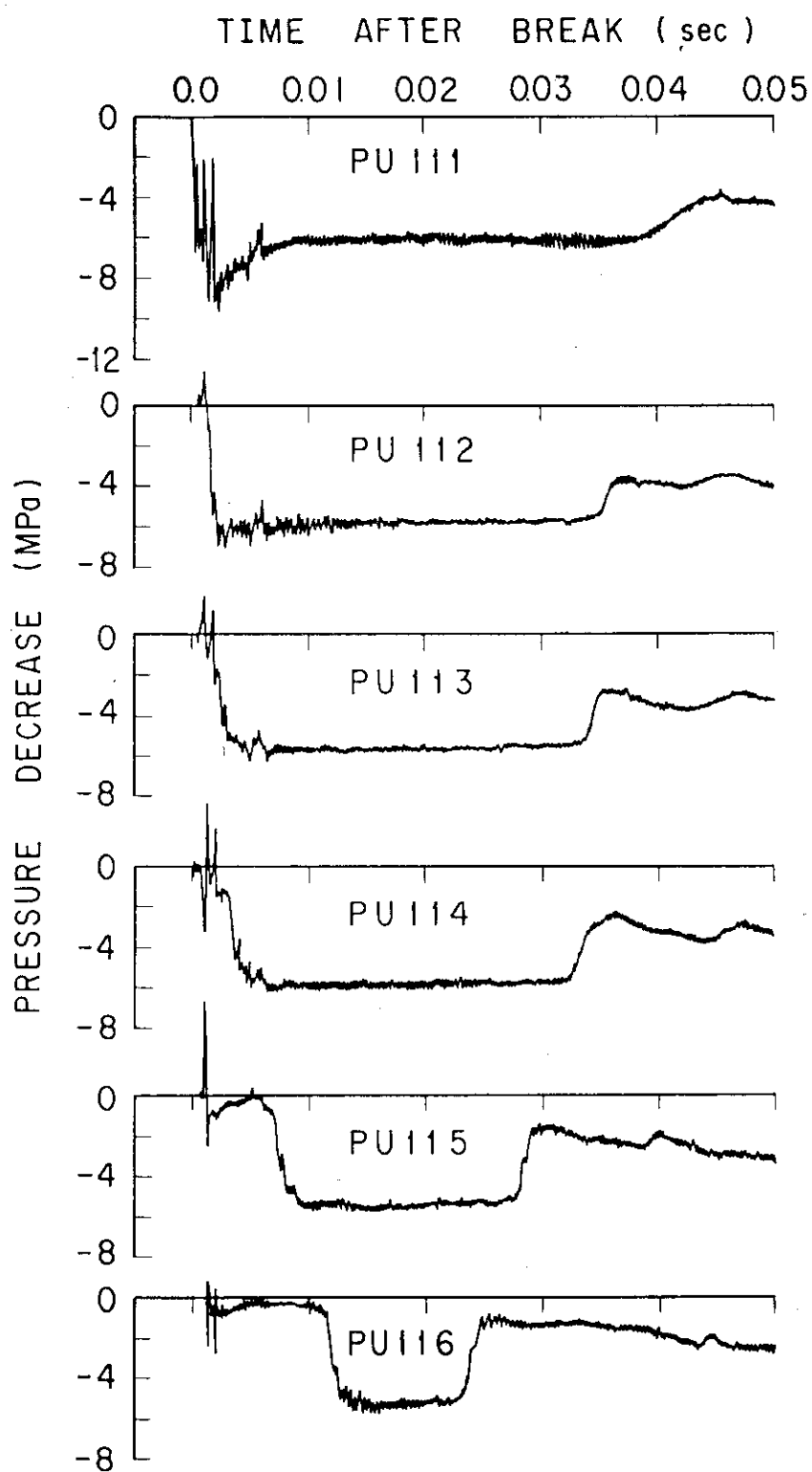


Fig. 4.3 Pressure histories in the test pipe and the vessel

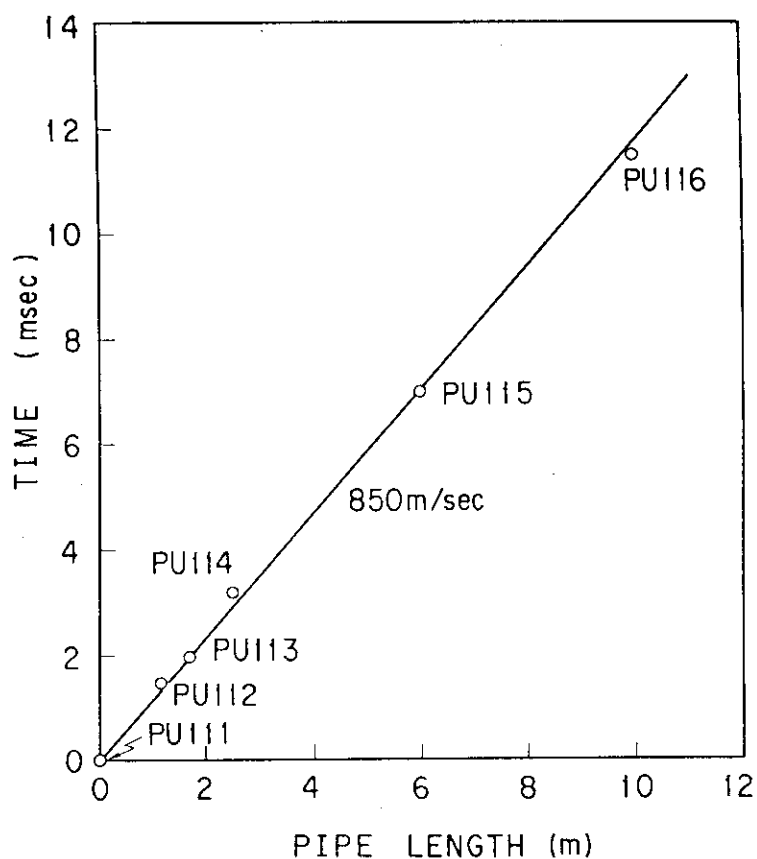


Fig. 4.4 Propagation of decompression wave in the test pipe

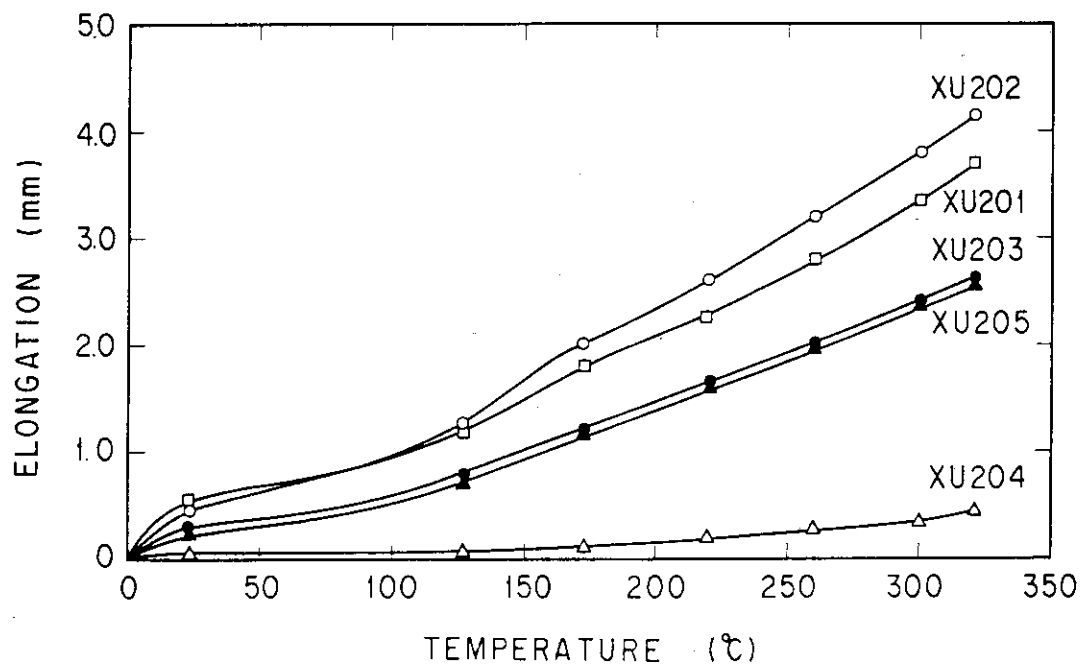


Fig. 4.5 Thermal expansion of the test pipe vs. temperature in RUN 5808

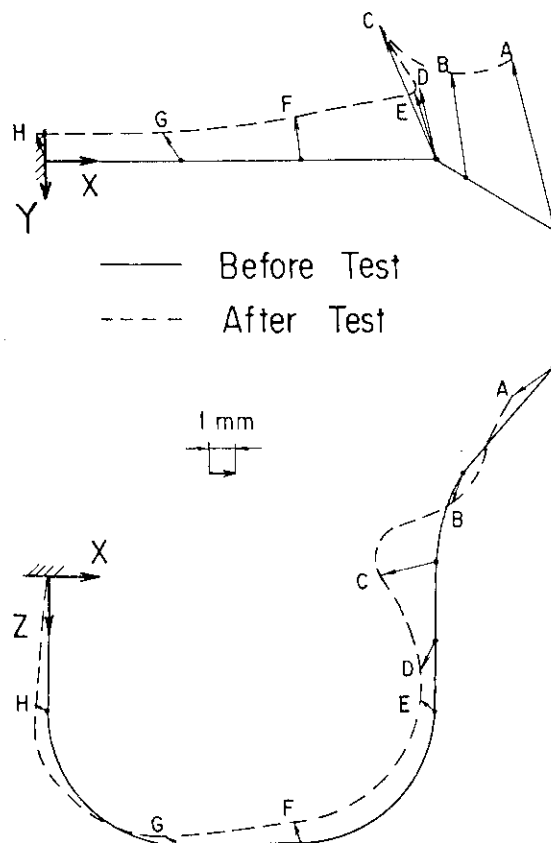


Fig. 4.6 Residual deformation of the test pipe after the test RUN 5809

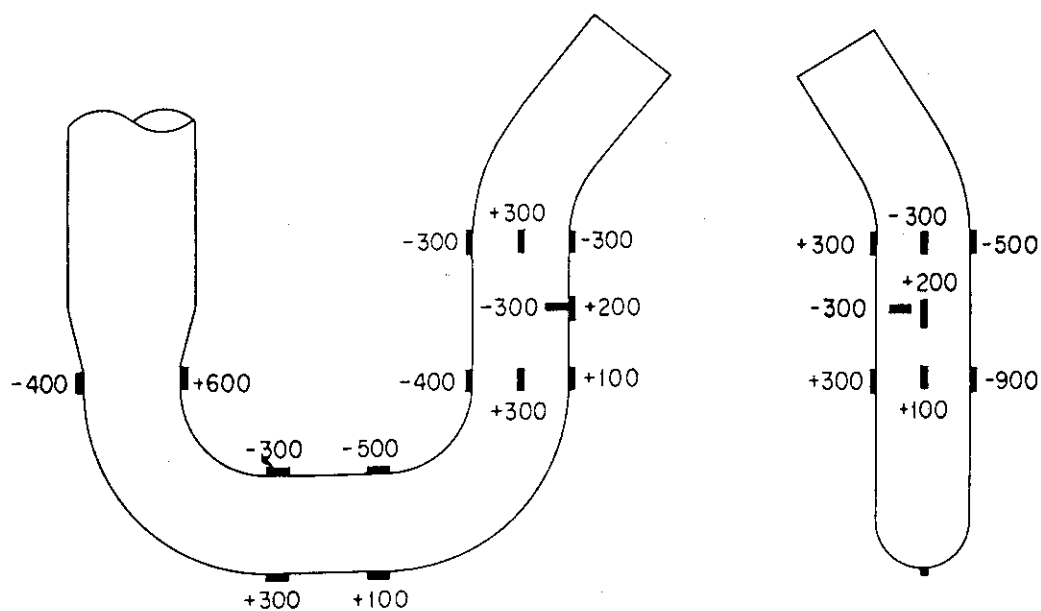


Fig. 4.7 Maximum strain values of the strain gages mounted on the test pipe

5. CONCLUDING REMARKS

Pipe whip test using 1/6 model of the cross-over leg piping in the primary loop of PWR plants was performed under the PWR LOCA conditions (325 °C, 15.7 MPa). The following results were obtained from this test.

- (1) Three restraints are adequately arranged to the test pipe, since the deformation of the test pipe is negligible after the test.
- (2) Velocity of pressure wave propagating in the water becomes about 850 m/sec, which is almost equal to the velocity of sound in the subcooled water with 15.6 MPa pressure.
- (3) Acceleration of the free end of the test pipe becomes more than 500 G just after the break.

ACKNOWLEDGEMENTS

The authors wish to make their grateful acknowledgement to the members of committee on the assessment of Safety Research for Nuclear Reactor Structural Components at JAERI (Chairman: Professor Emeritus Y. Ando, University of Tokyo), for their fruitful comments. Acknowledgement is also due to Dr. K. Sato, Director, and Dr. T. Shimooke, Duputy Director, of Department of Reactor Safety Research at JAERI for their great supports.

REFERENCES

- (1) N. Miyazaki, et al., "Pipe Rupture Test Results: 4-inch Pipe Whipping Tests under PWR LOCA Conditions (RUN No. 5506, 5507, 5508, 5604)", JAERI-M 82-125 (1982).
- (2) R. Kurihara, et al., "Pipe Rupture Test Results; 4-Inch Pipe Whip Test under BWR LOCA Conditions---Overhang Length Parameter Tests (RUN 5407, 5501, 5504, 5603), JAERI-M 82-022 (1982).
- (3) H. Hata, T. Kitamura, "Structural Design of Nuclear Components", Vol. 19 No. 6 Mitubishi Juko Giho (1982).

5. CONCLUDING REMARKS

Pipe whip test using 1/6 model of the cross-over leg piping in the primary loop of PWR plants was performed under the PWR LOCA conditions (325 °C, 15.7 MPa). The following results were obtained from this test.

- (1) Three restraints are adequately arranged to the test pipe, since the deformation of the test pipe is negligible after the test.
- (2) Velocity of pressure wave propagating in the water becomes about 850 m/sec, which is almost equal to the velocity of sound in the subcooled water with 15.6 MPa pressure.
- (3) Acceleration of the free end of the test pipe becomes more than 500 G just after the break.

ACKNOWLEDGEMENTS

The authors wish to make their grateful acknowledgement to the members of committee on the assessment of Safety Research for Nuclear Reactor Structural Components at JAERI (Chairman: Professor Emeritus Y. Ando, University of Tokyo), for their fruitful comments. Acknowledgement is also due to Dr. K. Sato, Director, and Dr. T. Shimooke, Deputy Director, of Department of Reactor Safety Research at JAERI for their great supports.

REFERENCES

- (1) N. Miyazaki, et al., "Pipe Rupture Test Results: 4-inch Pipe Whipping Tests under PWR LOCA Conditions (RUN No. 5506, 5507, 5508, 5604)", JAERI-M 82-125 (1982).
- (2) R. Kurihara, et al., "Pipe Rupture Test Results; 4-Inch Pipe Whip Test under BWR LOCA Conditions---Overhang Length Parameter Tests (RUN 5407, 5501, 5504, 5603), JAERI-M 82-022 (1982).
- (3) H. Hata, T. Kitamura, "Structural Design of Nuclear Components", Vol. 19 No. 6 Mitubishi Juko Giho (1982).

5. CONCLUDING REMARKS

Pipe whip test using 1/6 model of the cross-over leg piping in the primary loop of PWR plants was performed under the PWR LOCA conditions (325 °C, 15.7 MPa). The following results were obtained from this test.

- (1) Three restraints are adequately arranged to the test pipe, since the deformation of the test pipe is negligible after the test.
- (2) Velocity of pressure wave propagating in the water becomes about 850 m/sec, which is almost equal to the velocity of sound in the subcooled water with 15.6 MPa pressure.
- (3) Acceleration of the free end of the test pipe becomes more than 500 G just after the break.

ACKNOWLEDGEMENTS

The authors wish to make their grateful acknowledgement to the members of committee on the assessment of Safety Research for Nuclear Reactor Structural Components at JAERI (Chairman: Professor Emeritus Y. Ando, University of Tokyo), for their fruitful comments. Acknowledgement is also due to Dr. K. Sato, Director, and Dr. T. Shimooke, Deputy Director, of Department of Reactor Safety Research at JAERI for their great supports.

REFERENCES

- (1) N. Miyazaki, et al., "Pipe Rupture Test Results: 4-inch Pipe Whipping Tests under PWR LOCA Conditions (RUN No. 5506, 5507, 5508, 5604)", JAERI-M 82-125 (1982).
- (2) R. Kurihara, et al., "Pipe Rupture Test Results; 4-Inch Pipe Whip Test under BWR LOCA Conditions---Overhang Length Parameter Tests (RUN 5407, 5501, 5504, 5603), JAERI-M 82-022 (1982).
- (3) H. Hata, T. Kitamura, "Structural Design of Nuclear Components", Vol. 19 No. 6 Mitubishi Juko Giho (1982).